

Summary Report
1 June 1967 to 31 May 1969

GAS GUN FOR IMPACT STUDIES

G. R. Fowles, G. E. Duvall, J. Asay, P. Bellamy,
F. Feistmann, D. Grady, T. Michaels & R. Mitchell

Contract No.
F44620-67-C-0087

WSU SDL 69-02
June 1969

Research sponsored by the U.S. Air Force
Office of Scientific Research (Advanced Research
Projects Agency), Arlington, Virginia

SUMMARY REPORT

1 June 1967 to 31 May 1969

ARPA Order Number:	985
Program Code Number:	7D10
Name of Contractor:	Washington State University
Date of Contract:	1 June 1967
Amount of Contract:	\$194,341.00
Contract Number:	F44620-67-C-0087
Principal Investigator:	Professor George E. Duvall Phone: (509) 335-3310
Contract Expiration Date:	31 May 1969
Project Scientist:	Professor G. Richard Fowles Phone: (509) 335-4673
Title:	Material Behavior in High Speed Impact

GAS GUN FOR IMPACT STUDIES

G. R. Fowles, G. E. Duvall, J. Asay, P. Bellamy,
F. Feistmann, D. Grady, T. Michaels & R. Mitchell

ABSTRACT

A detailed description of the four-inch gas gun that has been designed and installed at Washington State University is presented. The design velocity is $1.4 \text{ mm}/\mu\text{s}$; the maximum velocity achieved to date is $0.9 \text{ mm}/\mu\text{s}$ with a 1100 gm projectile. Angular misorientation of the projectile with respect to the target surface is consistently below 0.5 milliradian. Brief descriptions of ancillary instrumentation and equipment are given and research problems under investigation in the areas of phase transformations and constitutive relations are discussed.

I. INTRODUCTION

This paper describes the gas gun and associated instrumentation that has been designed and installed at Washington State University. The first year of the two-year program was spent in design and construction of the gun.¹ It was installed at the beginning of the second year, and active research began some three months later after a number of shakedown experiments and minor modifications of the gun.

A gas gun was chosen as the principal experimental tool of the Shock Dynamics Laboratory for several reasons. These devices are capable of very precisely controlled impacts in which initial conditions of the projectile and target are well determined. Their velocity range (up to about 1.5 mm/ μ s) is adequate for the study of a wide range of physical phenomena including, for example, the study of phase transformations and constitutive relations. They are relatively safe and can be operated by a small number of personnel in a campus environment.

Although powder-driven guns can be shorter for a given projectile velocity, and are therefore less expensive, they are less suitable for precision impact studies because of problems of cleanliness and high recoil forces. Further, the problems of storage and handling of gunpowder in a campus environment, while not insurmountable, are substantial inconveniences.

Some of the conceptual design considerations leading to the choice of length, diameter, operating pressure, and mode of operation are discussed in Section II. Section III includes detailed descriptions of the major features, and Section IV describes the instrumentation developed for use with the gun. Sections V and VI describe the performance of the gun and some of the current research problems.

II. DESIGN CONSIDERATIONS

The major design parameters are length, diameter, operating pressure, and gas reservoir volume.

Projectile diameter is probably the most important parameter. Good measurements of plane stress wave propagation can be obtained only while the stress wave is accurately one-dimensional, i. e. before any signal from the lateral edges of the sample under investigation can influence the measurement. This restriction requires that the ratio of diameter to thickness of the sample be at least three and preferably four or more. If sample thicknesses up to one inch are to be studied, or if it is desired to compare two or more thinner samples under identical impact conditions, a projectile diameter of about 4 inches is necessary. The experience of other investigators with guns varying between 2.5 and 6 inches indicates that these are reasonable limits;²⁻⁴ a six-inch gun, however, is expensive to build and to operate. We therefore decided on a diameter of 4 inches as the maximum that is practicable within the bounds of reasonable construction and operating costs.

The length was chosen to some extent on the basis of available space, with consideration given also to desired projectile velocities and operating pressures.

At 6000 psi operating pressure, which is a convenient limit in terms of availability of compressors, gauges, and tubing, a barrel length of more than about fifty feet does not materially increase the attainable projectile velocities. The length chosen for the gun was 14 meters in order to fit conveniently into the room available. Figure 1 shows the projectile velocity as a function of barrel length for various values of the ratio of mass of driven gas to projectile mass. The length chosen for the gun is clearly well beyond the knee of these curves and is sufficient to extract nearly all the velocity possible from a given reservoir at the maximum operating pressure (6000 psi).

The gas reservoir volume was chosen to give a maximum ratio of mass of gas to projectile mass (G/M) of about five. The maximum velocity increases very slowly with G/M beyond this value, as shown in Fig. 2, and

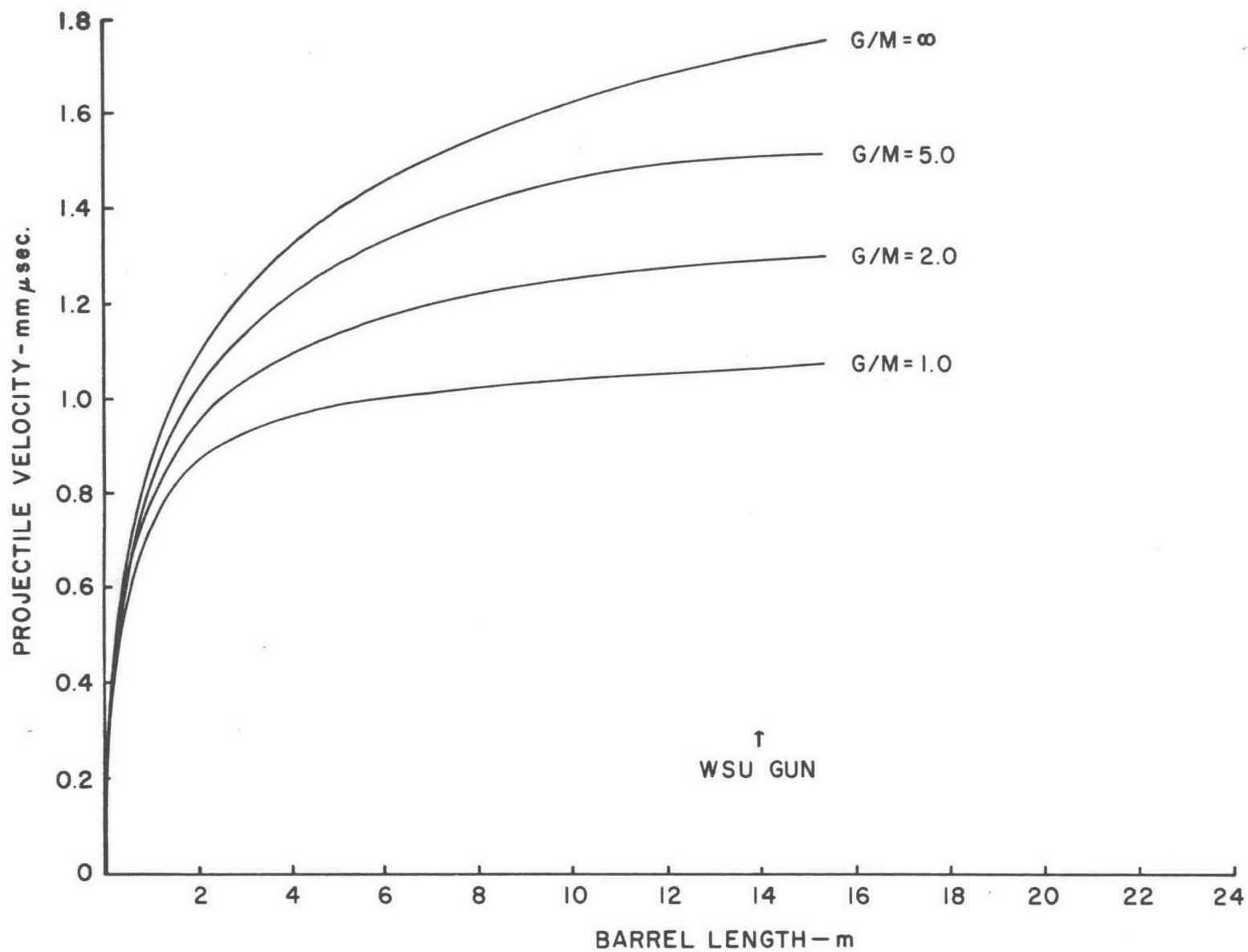


Fig. 1. Projectile velocity as function of barrel length for various ratios of mass of gas, G, to mass of projectile, M. Helium gas. (After Siegel⁵)

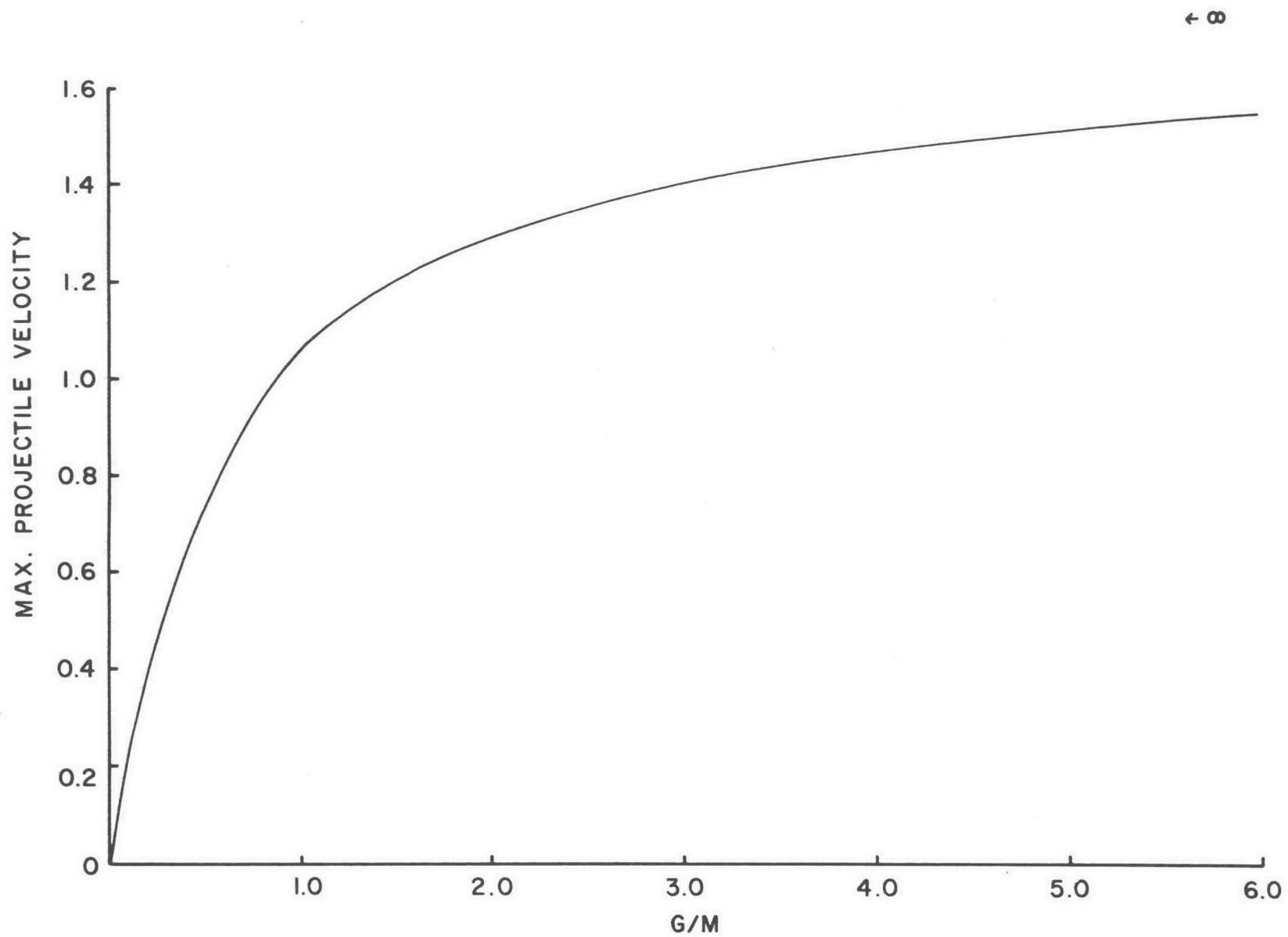


Fig. 2. Maximum projectile velocity as a function of G/M for 14 m barrel. Helium gas. (After Siegel⁵)

higher reservoir volumes increase the cost of gas which, in the case of helium, is not trivial. For projectile masses of 450 gm, which is about the minimum weight that can be fired with adequate strength and rigidity, the corresponding reservoir volume for Helium at 6000 psi is one cubic foot and this value was therefore adopted. The curves shown in Figs. 1 and 2 were taken from Siegel,⁵ and were verified by similar calculations in this laboratory by Richard White.⁶

Thus, within the bounds of reasonable practicality the gun is designed to give nearly the maximum velocity (~ 1.5 mm/ μ s) and maximum diameter attainable in a single stage gun. Improved performance would result from use of hydrogen, but this gas was ruled out because of handling and safety problems.

Aside from the choice of operating parameters indicated above the most important feature of the gun is the method for absorbing recoil. Detailed gas dynamical calculations indicate a maximum momentum of about 2×10^8 dyne-sec, and a maximum unbalanced force of 75,000 pounds.⁶

It was decided, rather than to attempt to hold the gun rigidly with the target fastened to the barrel, to let the gun slide freely while holding the target stationary. By this means the recoil forces are substantially reduced and can be accommodated by standard shock absorbers. This has the additional advantage that no appreciable vibrations are transmitted to the target from the barrel. The principal concern with this scheme is whether or not sufficient control can be maintained of the tilt of the projectile with respect to the target. It is necessary to maintain the tilt below about one milliradian in order not to cause degradation of the time resolution available from recording techniques. Consideration of the possible extent of misalignment during the approximately one-inch of motion of the gun barrel before impact indicated, however, that significant bending or rotation would not be expected.⁷ This conclusion has been subsequently verified by tilt measurements that are consistently below 0.5 milliradians, and are frequently much less.

Other desirable features of the design are (1) capability for evacuating all sides of the target to avoid distortion, (2) breech mechanisms which can be precisely triggered and have fast opening times, and (3) quiet operation.

The breech mechanisms are described in detail in Section III. Two interchangeable breeches with different projectile firing mechanisms were designed and built because no single breech of an existing gun performs optimally throughout the desired velocity range (~ 0.1 to 1.5 mm/ μ s). Several new concepts for a breech design that would accommodate the complete velocity range were considered, but were rejected in favor of two breeches on the basis of simplicity and reliability.

The desirability of fast breech opening times was shown by computer simulation studies performed by Richard White.⁸ The results are shown in Fig. 3 and clearly indicate that, for maximum performance, the breech mechanism must provide unrestricted gas flow within a few milliseconds.

The low pressure breech (to 3000 psi) is of the wrap-around type developed by Muhlenweg at Sandia Corporation. This design is very convenient to use, employs no moving parts under pressure except the projectile itself, and is automatically fast-opening. Its only disadvantage is that the projectile must be strong enough to withstand the initial pressure and, therefore, the projectile mass is larger than would otherwise be required. Hence, the maximum velocity attainable is reduced.

To circumvent this limitation at higher pressures (to 6000 psi) a double-diaphragm breech was also built, also patterned after a Sandia design. It imposes no limitation on projectile weight, but is more expensive and less convenient to operate since two burst diaphragms must be inserted into the breech for each shot.

It is expected that the bulk of the research to be performed immediately with the gun will use the wrap-around breech and will be limited to velocities below about 1.0 mm/ μ s. The double-diaphragm breech is available, however, for work at higher velocities.

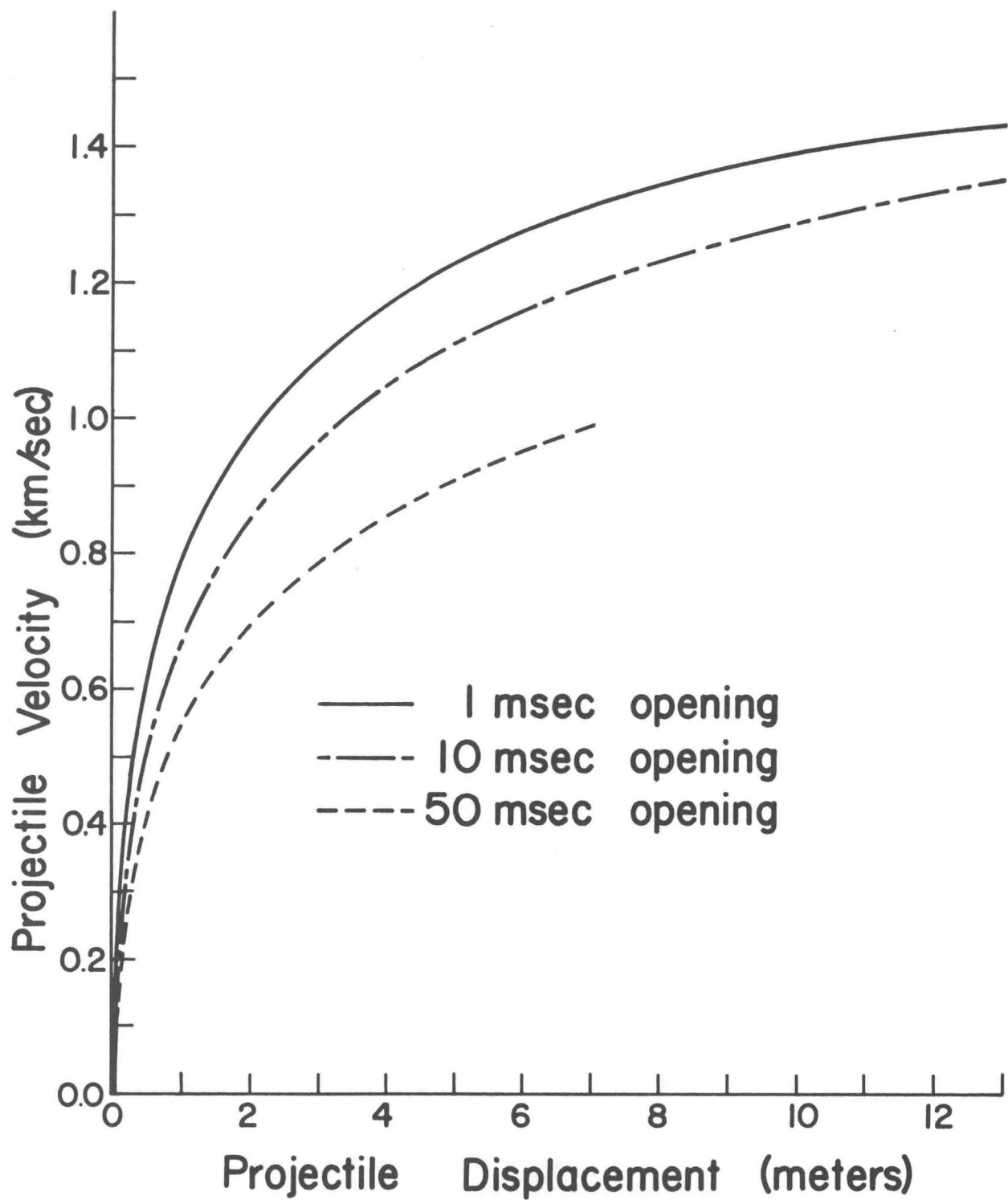


Fig. 3. Projectile velocity in the WSU gas gun as function of projectile displacement for three valve-opening times.

There was substantial concern about the acoustic noise produced by the gun inasmuch as it is located directly below a large lecture room. Partly to help control noise, and partly for safety purposes, a catcher tank was constructed that contains all of the fragments and the gas. This tank, which incorporates a large evacuated target area, and the heavy concrete shielding around the muzzle reduce the noise to surprisingly low levels. We have been able to fire, at pressures up to 3000 psi so far, without disturbing classes in the room above.

III. DESIGN DETAILS

A. Location

The room in which the gun facility is located is a basement room in a large classroom and office building on the WSU campus - Sloan Hall. It is approximately 75' x 25' and is partially below ground level. Inside this room we constructed a very heavy, reinforced concrete muzzle room approximately 11' x 16' x 7'. The walls, ceiling and floor are reinforced and are 12" thick. The door is $\frac{1}{2}$ " thick steel plate and weighs 600 pounds. This room was designed to withstand the maximum overpressure of the gas in case of rupture of the catcher tank (approximately 4 psi).

Concrete blocks with reinforcing rods were used to shield the breech and compressor room from the central part of the main room. The central portion, between the breech and muzzle rooms, is used as a working area and houses the instrumentation and the control console.

A sketch of the layout is shown in Fig. 4.

The gun is mounted on an I-beam, which in turn rests on a solid concrete foundation.

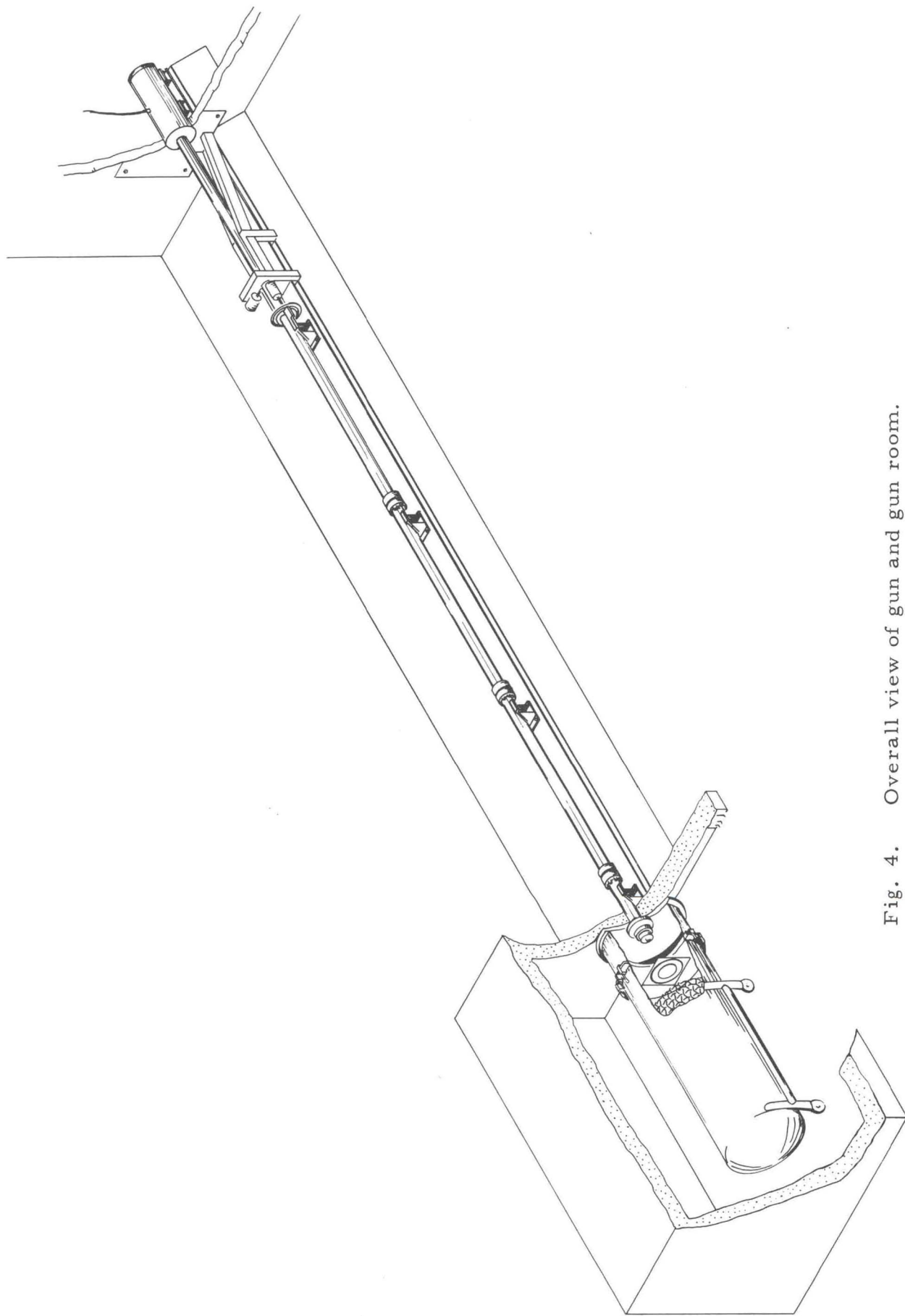


Fig. 4. Overall view of gun and gun room.

B. Barrel

The barrel is constructed in four ten-foot sections and one four-foot muzzle section. It was drilled from 4140 HT steel heat-treated to 38 Rockwell C. The sections have bayonet joints at each end and are held together with flanges threaded onto each barrel section with buttress threads (Fig. 5). The flanges are in turn bolted together with eight 3/4", high strength (UNBRAKO) cap screws.

The inside diameter of the barrel is 4.001 ± 0.001 "; the muzzle section tapers slightly from 4.001 to 4.0005" over the last 12". This taper was initially greater but was honed out after test firings indicated excessive friction in the tapered section.

C. Barrel Supports

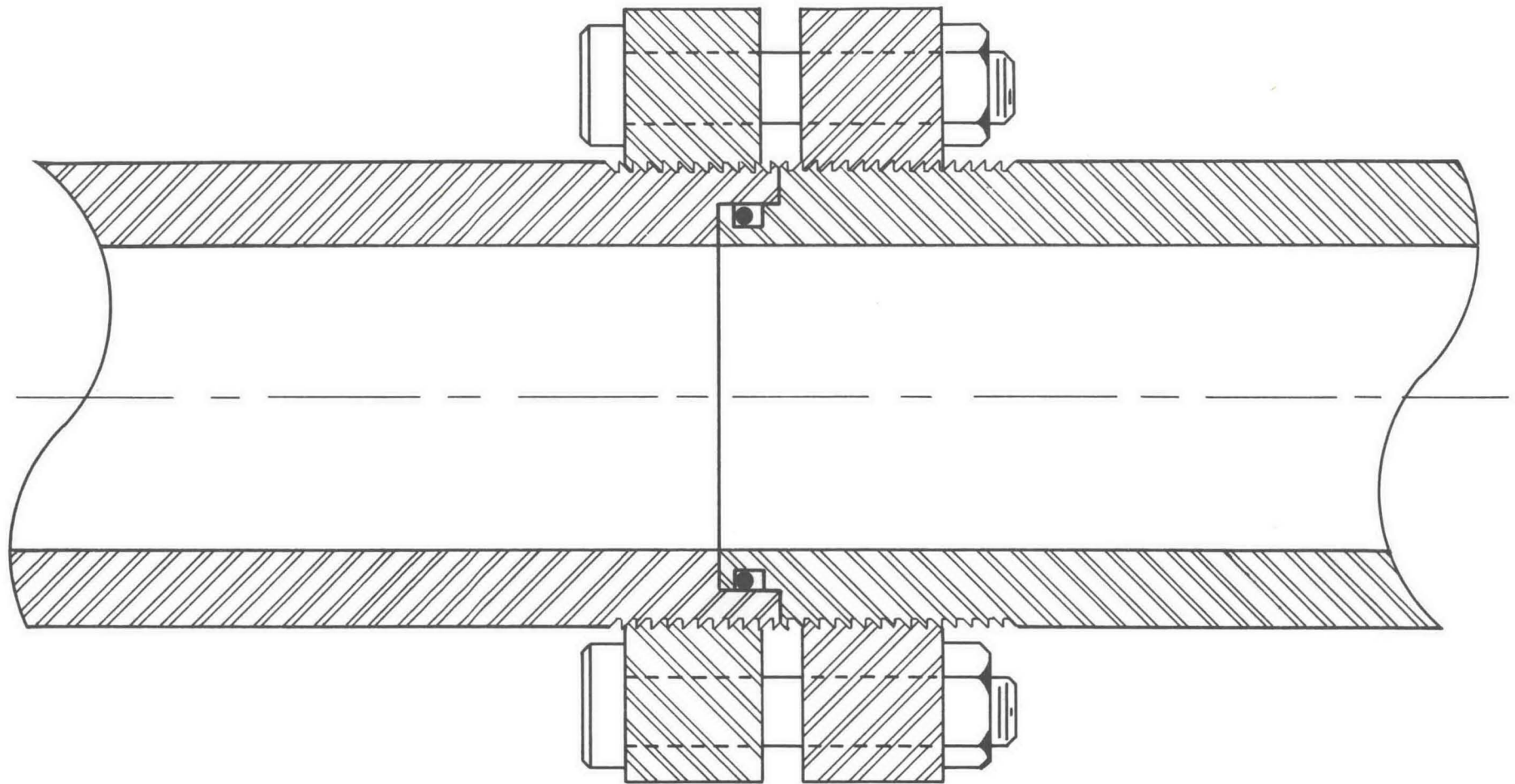
It was decided to maintain the barrel as torque-free as possible while the projectile was in the gun. Consequently, the barrel rests only on oiled porous bronze bearings constructed as caps for bolts threaded through V-blocks (Fig. 6). These are located at ten-foot intervals along the gun. Although some sagging of the barrel between supports occurs, it has not proved to be necessary to add more supports.

The muzzle of the gun protrudes into the muzzle room; a vacuum and pressure seal is provided by a brass bushing and O-ring. Initially this bushing was made of steel but it was found to seize to the barrel on occasion. No problems have been experienced with the brass bushing.

D. Breeches

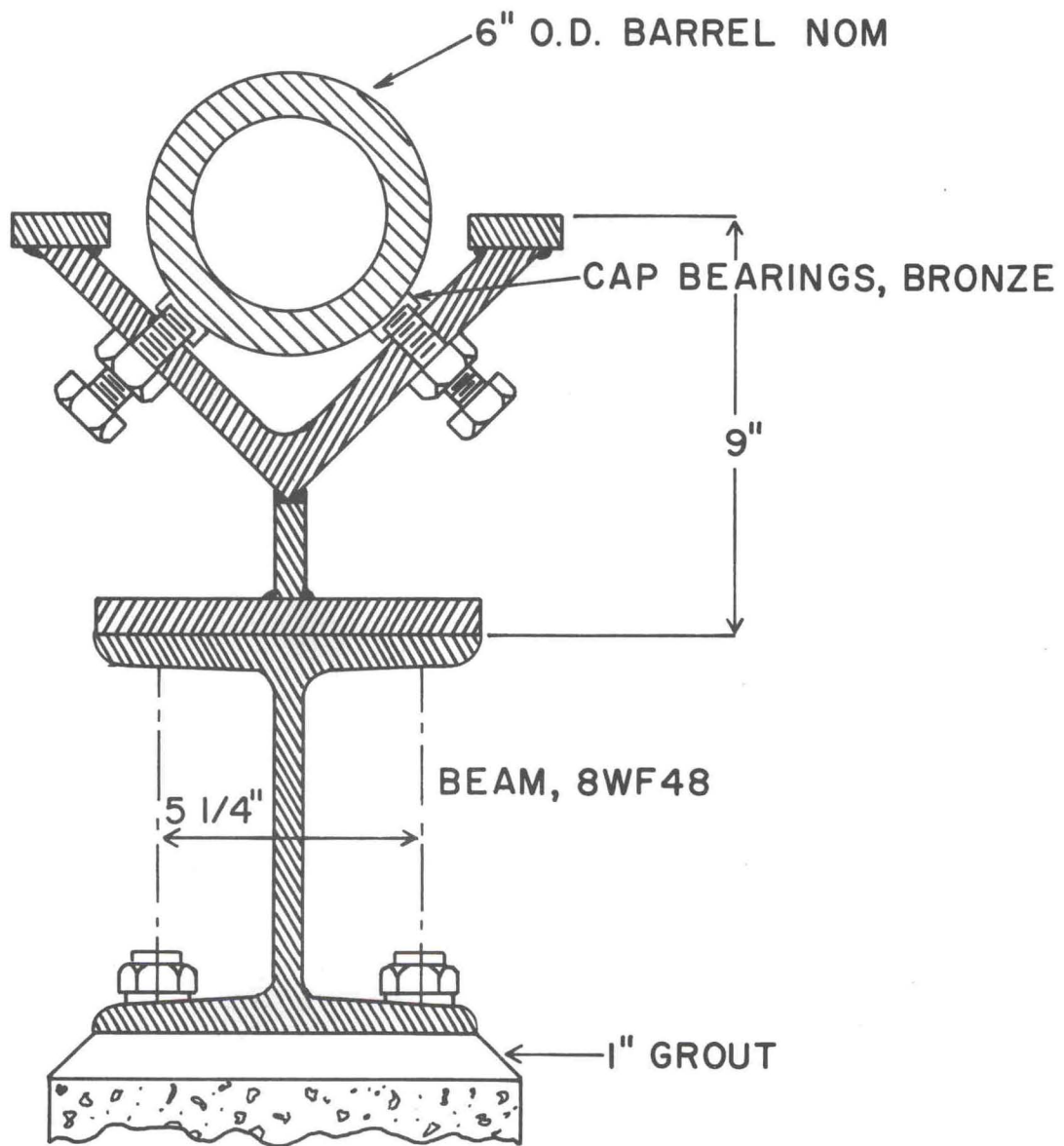
Diagrams of the two interchangeable breeches are shown in Figs. 7 and 8. Each contains one cubic foot of gas; the wrap-around model is designed for 6000 psi. They have been tested to 6000 and 10,000 psi, respectively.

In the wrap-around design the projectile seals the ports between the barrel and the annular reservoir by means of O-rings at each end of the projectile. Firing is accomplished by injecting a small amount of high pressure gas behind the projectile, causing it to move past the ports.



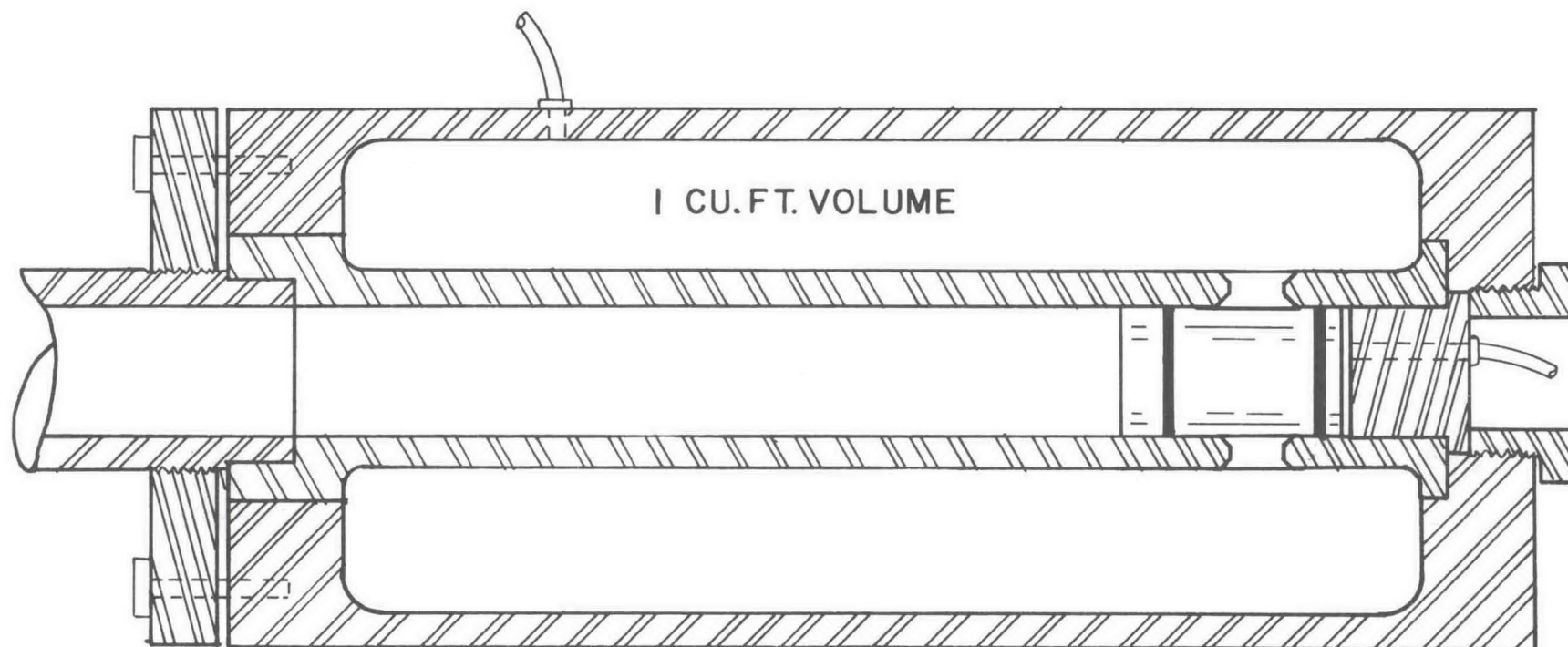
BAYONET BARREL JOINT CONNECTION

Fig. 5. Barrel joint detail.



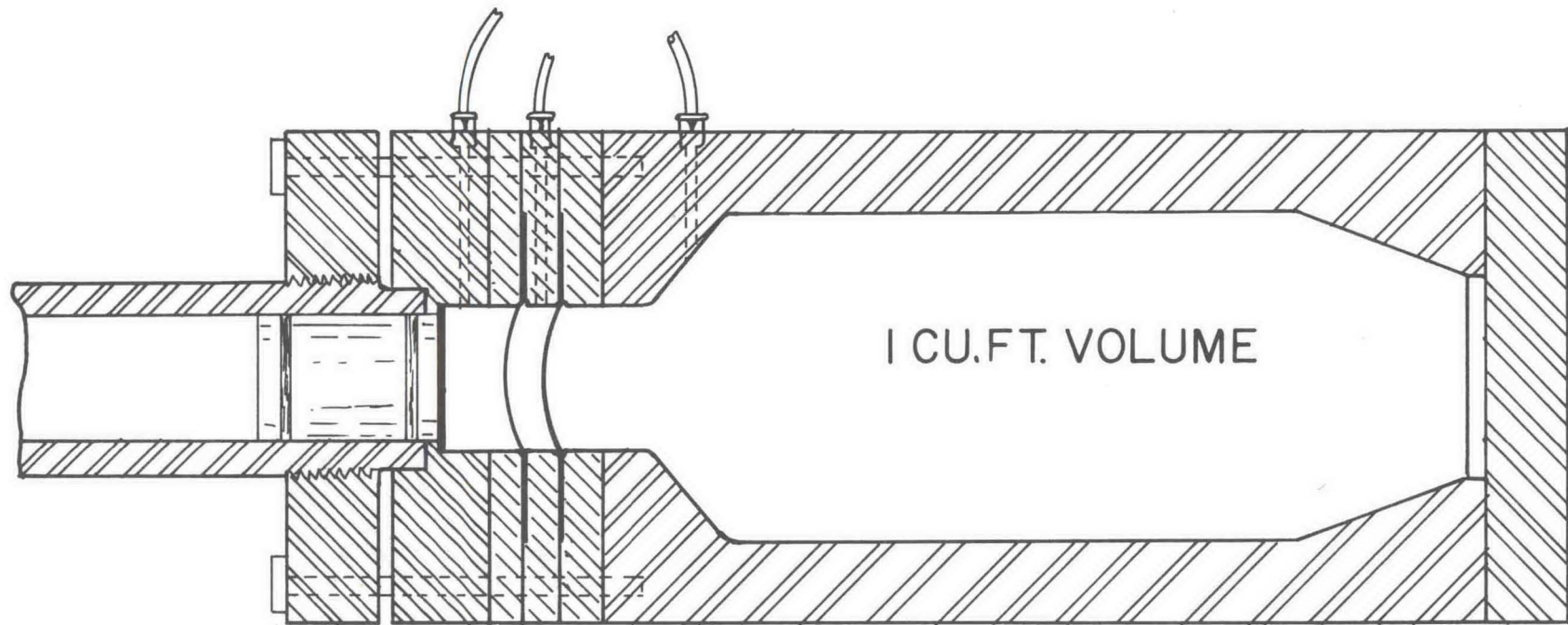
SCALE: 1/4"

Fig. 6. Barrel supports.



WRAP-AROUND BREECH ASSEMBLY

Fig. 7. Wrap-around breech assembly.



DOUBLE-DIAPHRAM BREECH ASSEMBLY

Fig. 8. Double-diaphragm breech assembly.

This design is convenient and reliable. Its only disadvantage is the restriction on projectile weight imposed by the requirement of sufficient strength to stand-off the initial pressure. The minimum projectile weight we have attempted with this breech is 1100 grams with a projectile constructed of 6061-T6 aluminum.

For the higher velocity range (~ 0.9 to 1.5 mm/ μ s) the double diaphragm breech is available. The diaphragms are selected to withstand half the reservoir pressure and to open cleanly and quickly when subjected to the full pressure. Firing is accomplished by exhausting the region between the diaphragms (initially pressurized to half pressure) so that each diaphragm in turn experiences the full pressure.

With this breech it is hoped that projectiles as small as about 450 grams can be fired. It has not been tested at the time of this writing but no serious problems are anticipated.

E. Projectiles

In order to reduce the costs of the projectiles it was decided to standardize on a design which would be usable for most of the shots and to have these made in quantity by a production shop (Fig. 9). The projectiles are machined from solid 6061-T6 aluminum so there are no joints to leak or fail when used in the wrap-around breech. Moreover, the Hugoniot of this material is well known so that impedance-match solutions can be readily obtained. The wall thickness was chosen to withstand an outside pressure of 3000 psi with a safety factor of 1.5; some of the projectiles have been tested to an outside pressure of 4500 psi.

The length of the projectiles is two diameters (8") and the outside diameter is $3.9975'' \pm \begin{matrix} .000'' \\ .005'' \end{matrix}$, which confines the maximum tilt to 0.5 milliradians or less when the projectile contacts the target (i. e. when the projectile protrudes two inches from the muzzle). The O-rings help to confine the projectile to the center of the barrel and close tolerances are held on these grooves, both in concentricity (.001 T.I.R.)

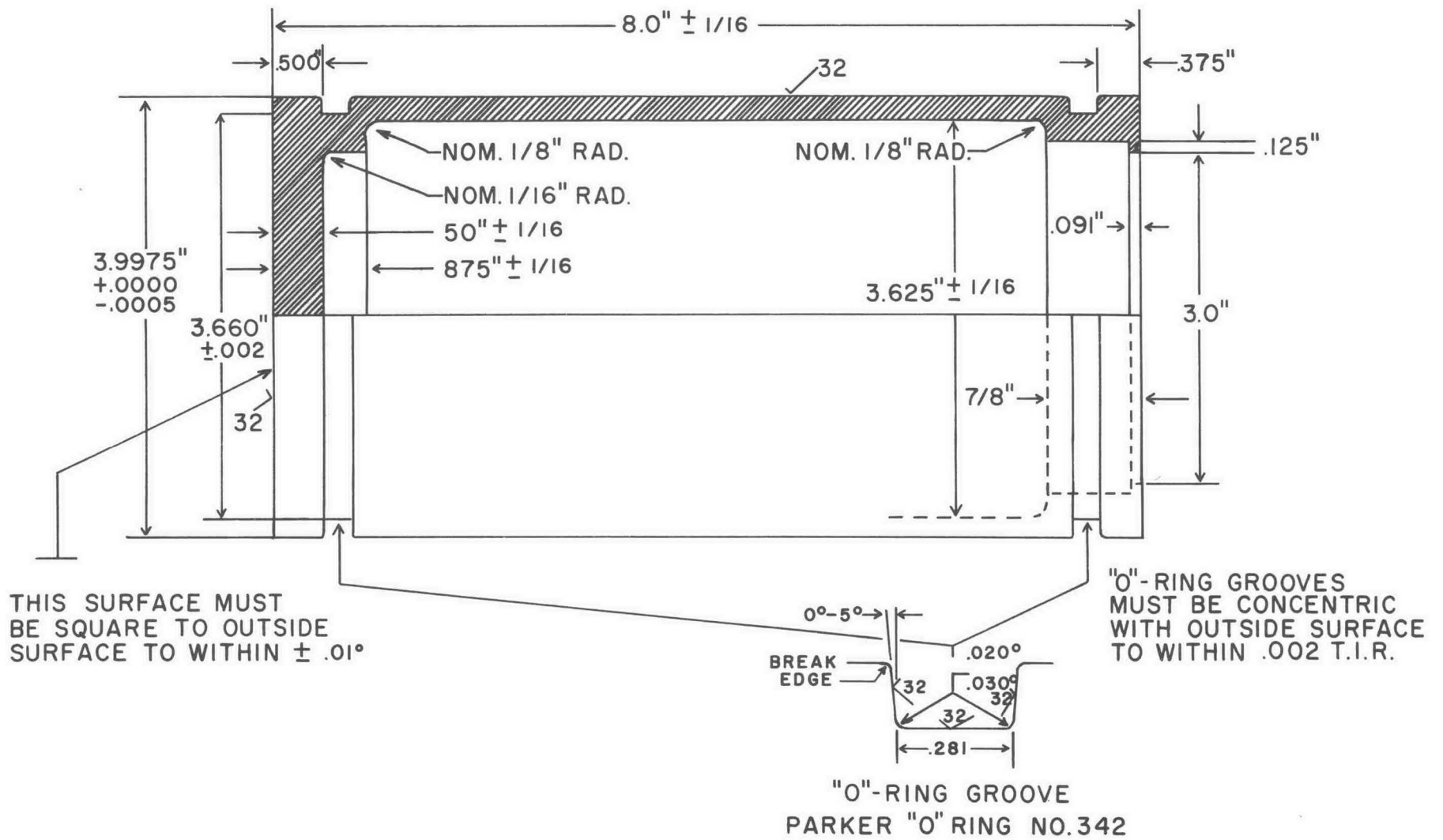


Fig. 9. Drawing of "standard" projectile. Material is 6061-T6 Aluminum.

and size ($\pm .001''$). The O-rings are teflon-coated Parker O-rings No. 2-342 made of Buna-N rubber with a 70 durometer hardness.

The projectile's weight is 1.1 kilograms. This limits the maximum velocity in the wrap-around breech to 0.6 mm/ μ s with nitrogen as the driver gas and 0.9 mm/ μ s with helium.

The impacting surface of the projectiles is lapped flat, and brought into square with the axis of the projectile, with a Lapmaster lapping machine. To check the impacting face for perpendicularity with respect to the axis of the projectile, the projectile is placed impacting-face down on a surface plate and rotated against a reference pin. A dial indicator measures any runout of the top with reference to the pin. The runout is kept within .0005". This means the impacting surface is perpendicular to the axis of the projectile to within 0.1 milliradians. Any deviation is removed during the lapping process by eccentrically weighting the projectile.

F. Recoil and Catcher System

The most unusual feature of the gun compared to others of its type is that it is allowed to recoil freely until after impact has occurred; after impact the gun is decelerated by velocity-sensitive shock absorbers. The target is mounted rigidly on the muzzle room wall and is therefore stationary. This arrangement essentially eliminates all problems of vibration of the target prior to impact. Further, standard shock absorbers can be used to stop the gun with maximum forces which are much less than the maximum unbalanced force on the gun during firing. Two shock absorbers of 15,000 inch-lb capacity and 3" travel bear against one of the barrel flanges and against a steel frame that transfers the momentum to the I-beam (Fig. 4).

The catcher tank consists of two sections. One section - the target chamber - is permanently mounted to the wall of the muzzle room (Fig. 4). This section is evacuated prior to the shot. The second section is mounted on casters and joins the first section by means of

quick-disconnect devices. This section contains the projectile-stopping mechanism and is not evacuated. A mylar diaphragm 18" in diameter and 0.005" thick provides an easily perforated seal between the two sections.

The projectile-stopping mechanism consists of a heavy wire cage, 18" in diameter and 8' long, stuffed with nylon or Dacron rags (Fig. 10). At the rear of the cage is welded a 4" thick by 24" diameter steel plate weighing 500 lbs; the total weight of the cage, rags, and steel plate is about 1000 lbs. This assembly is suspended on a rail and achieves a maximum velocity of about 2 m/sec when the maximum momentum of the projectile ($\sim 10^8$ dyne-sec) is absorbed by it. The force required to stop the assembly within 3 inches of travel is therefore less than 7000 lbs, and is accomplished with shock absorbers bearing against the rear of the tank.

G. Target Holder and Alignment Tools

The target holder is a ring with a lapped shoulder against which the target is held by small breakaway tabs (Fig. 11). Adjustment of the orientation of the target holder is accomplished with three differential screws that provide high strength and fine adjustment capability.

The tools used to align the target holder perpendicular to the axis of the barrel are a brass gauge plug and a gauging fixture which carries a sensitive dial indicator. The gauge plug is a fourteen inch solid brass bar with the diameter machined .001 to .0015" smaller than the exit diameter of the gun muzzle. A two-inch tapered section is machined on the leading end to facilitate fitting the plug into the barrel. The gauging face of the plug is flat and perpendicular to the axis to within .05 milliradians and is periodically checked with the same fixture used to check the projectiles. The gauge plug is solid to provide a heat sink so that handling does not change its dimensions or straightness.

The gauging fixture is simply a ring, ground flat, and large enough to mate onto the target aligning surface. A sensitive dial indicator is rigidly supported through the ring to sweep a three and one-half inch

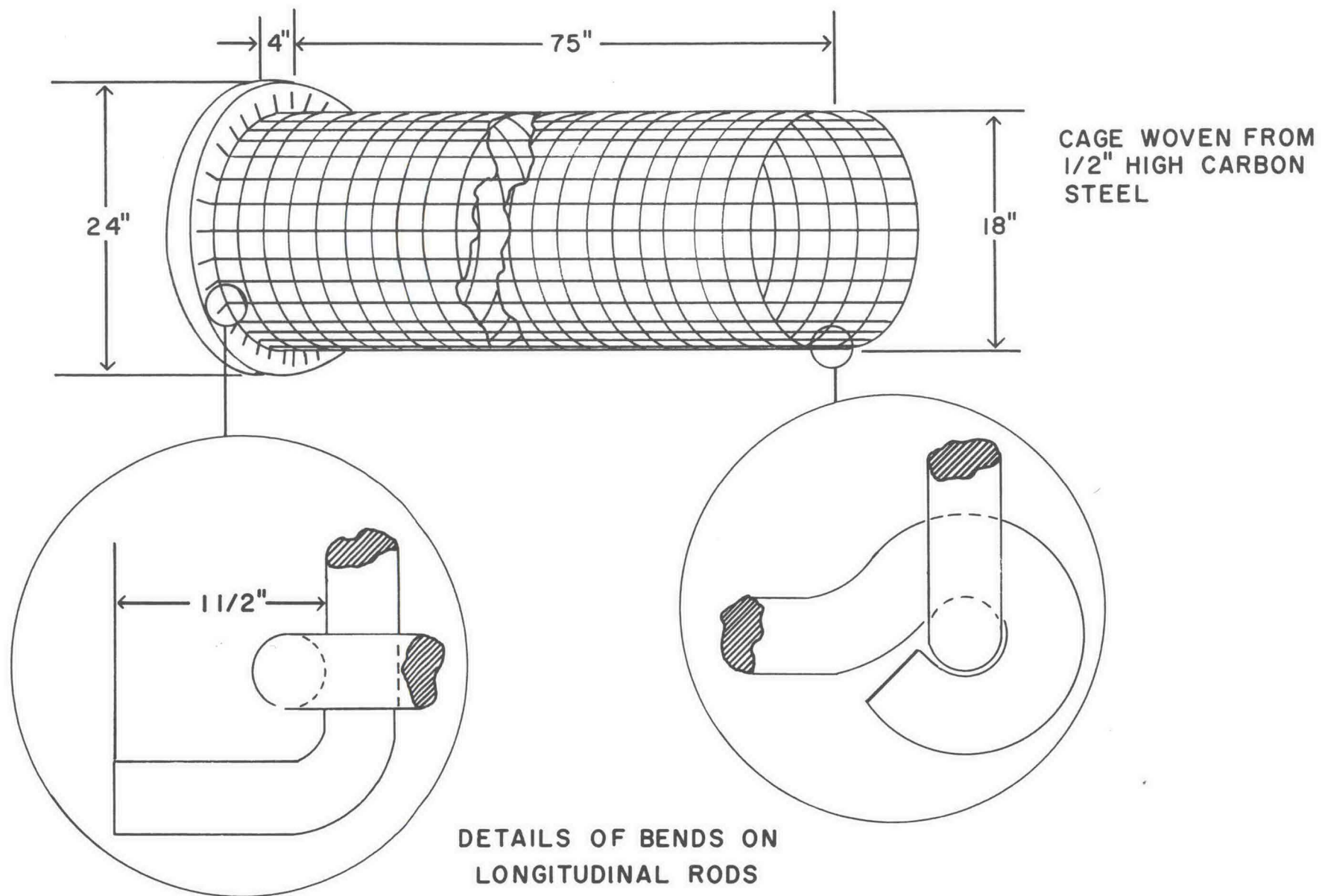


Fig. 10. Wire cage for stopping projectile. In operation the cage is stuffed with rags.

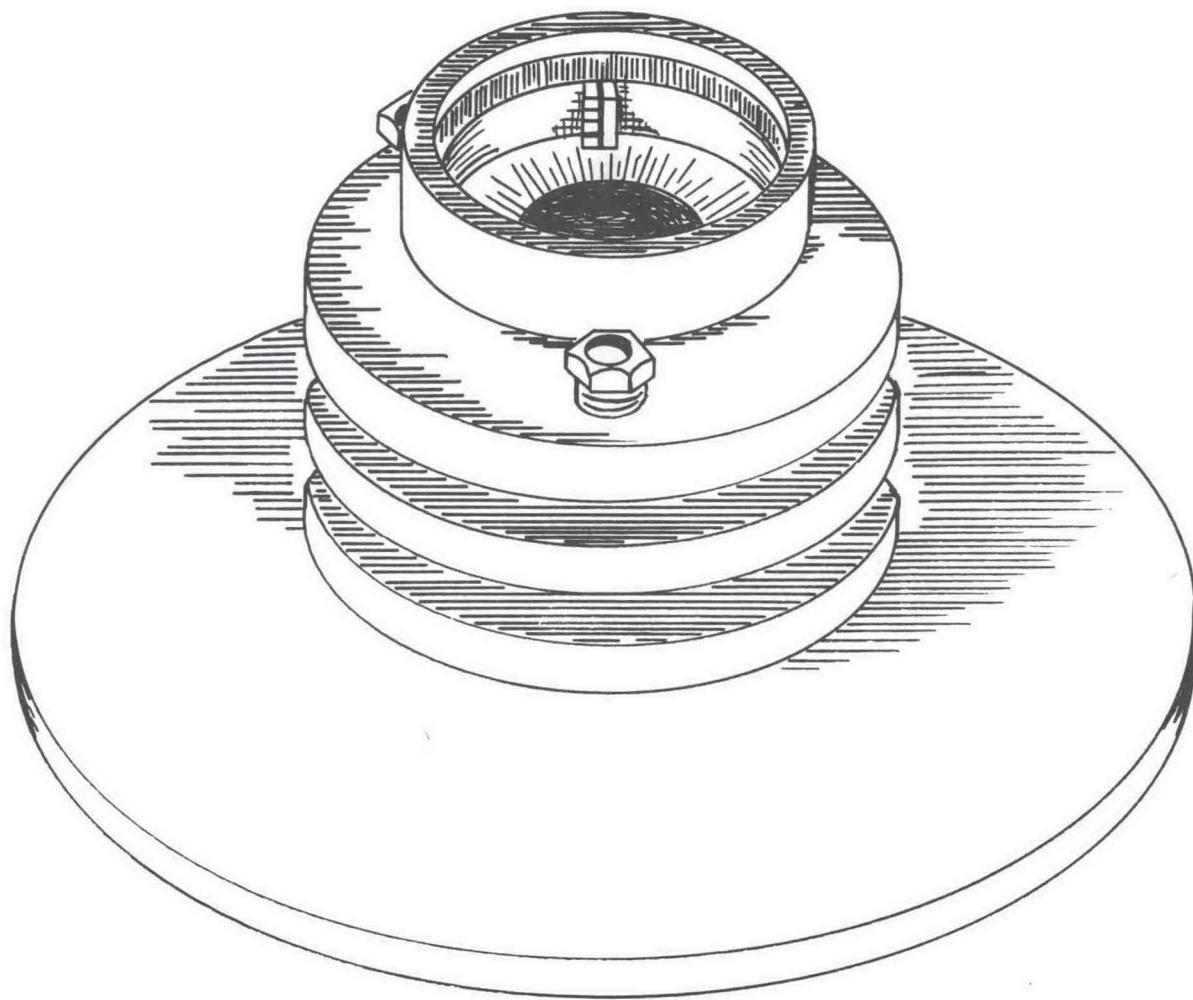


Fig. 11. Target holder.

diameter circle on the face of the gauge plug. It measures the change in distance between the plane of the target holder and the face of the gauge plug.

To align the target ring the gauge plug is positioned in the barrel and the gauging fixture is placed in the target holder and held with spring clips against the aligning surface. The dial indicator is then adjusted to touch the surface of the gauge plug and to give a null reading. The aligning fixture is then rotated and the dial indicator readings noted. The alignment nuts (differential nuts) are adjusted until a 360° rotation of the aligning fixture in both directions shows no greater than .0002" variation in readings. This corresponds to a misalignment of .06 milliradians or less. The gauge plug is then rotated and the alignment rechecked.

H. Projectile Velocity Pins

Projectile velocity is measured with a series of four pins, spaced one centimeter apart, which make electrical contact with the projectile. To insure a good ground each pin has a companion grounding pin which is positioned to make contact shortly before the active pin. The pins are machined from 1/16" brass rod; a whisker .010" in diameter and .10-.15" long is turned on one end. These eight pins are positioned in a block so that the projectile contacts one-third of the whisker length.

The velocity pin block is designed to insulate each of the active pins (velocity pins) from each other and from ground and to provide a BNC Connection for each (Fig. 12). The velocity pins are stair-stepped so that each pin makes contact with the projectile on fresh metal to insure accurate knowledge of spacing. The spacing of each pin pair is measured with a Gaertner toolmaker's microscope. The average of three sets of measurements yields an accuracy of ± 10 microns, or about .1%.

Shortly before firing the velocity pin block is slipped into a close-fitting hole in the target ring and the electrical connections are made.

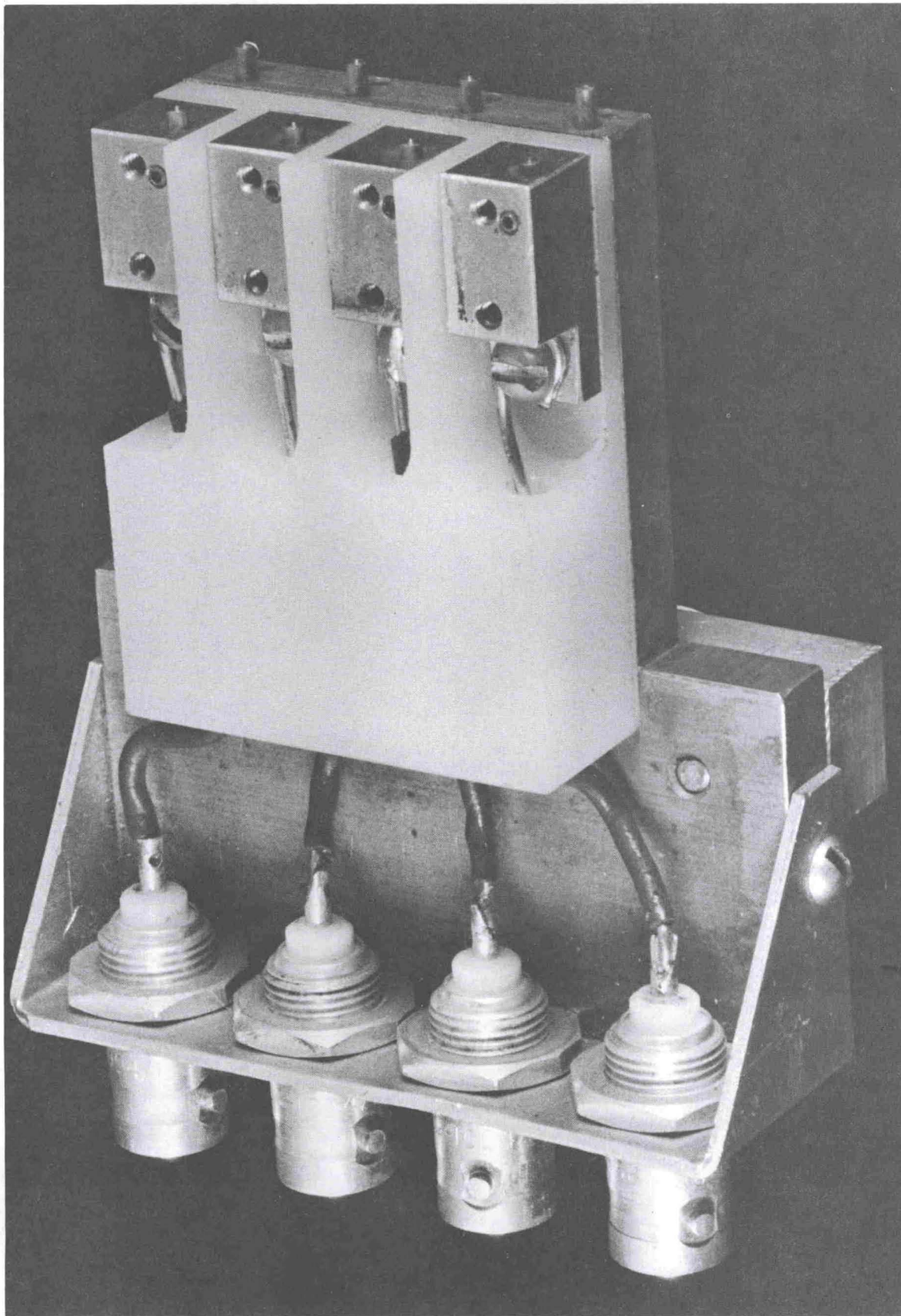


Fig. 12. Velocity pin holder.

The first velocity pin makes contact with the projectile at a distance of 3.5 centimeters in front of the target and triggers the velocity-measuring scope. The three intervals available provide redundant measurements of velocity and acceleration to provide a consistency check.

I. Control System

The control system was designed with the following criteria in mind:

- i) It must handle pressures up to 6000 psi remotely.
- ii) It must be essentially fail-safe, yet contain a minimum of interlocks.
- iii) It must indicate, at a glance from the operator, the complete status of the system at any time, particularly just before firing.
- iv) It must be easily adaptable to both breeches.

The above specifications were met by coupling two subsystems to the main high pressure system. A 110 VAC electrical system controls a low pressure (60 psi) air system, through the use of electrically operated three-way solenoid valves. These in turn control the actuators of the high pressure (6000 psi) valves.

1. High Pressure System (Fig. 13)

The high pressure system is built entirely of 1/4" OD x 7/64" ID 316 SS annealed tubing. Since the gas used as propellant is obtained from bottles it is desirable to allow for direct access to the breech reservoir from the bottles without first passing through the high pressure pump. This is done by laying a bypass line from the pump inlet to the outlet (Valve No. 18). A one-way check valve is inserted just before the entry of the bypass line into the high pressure side of the pump outlet to guard against the possibility of someone inadvertently opening the bypass valve when the system pressure is above 2000 psi.

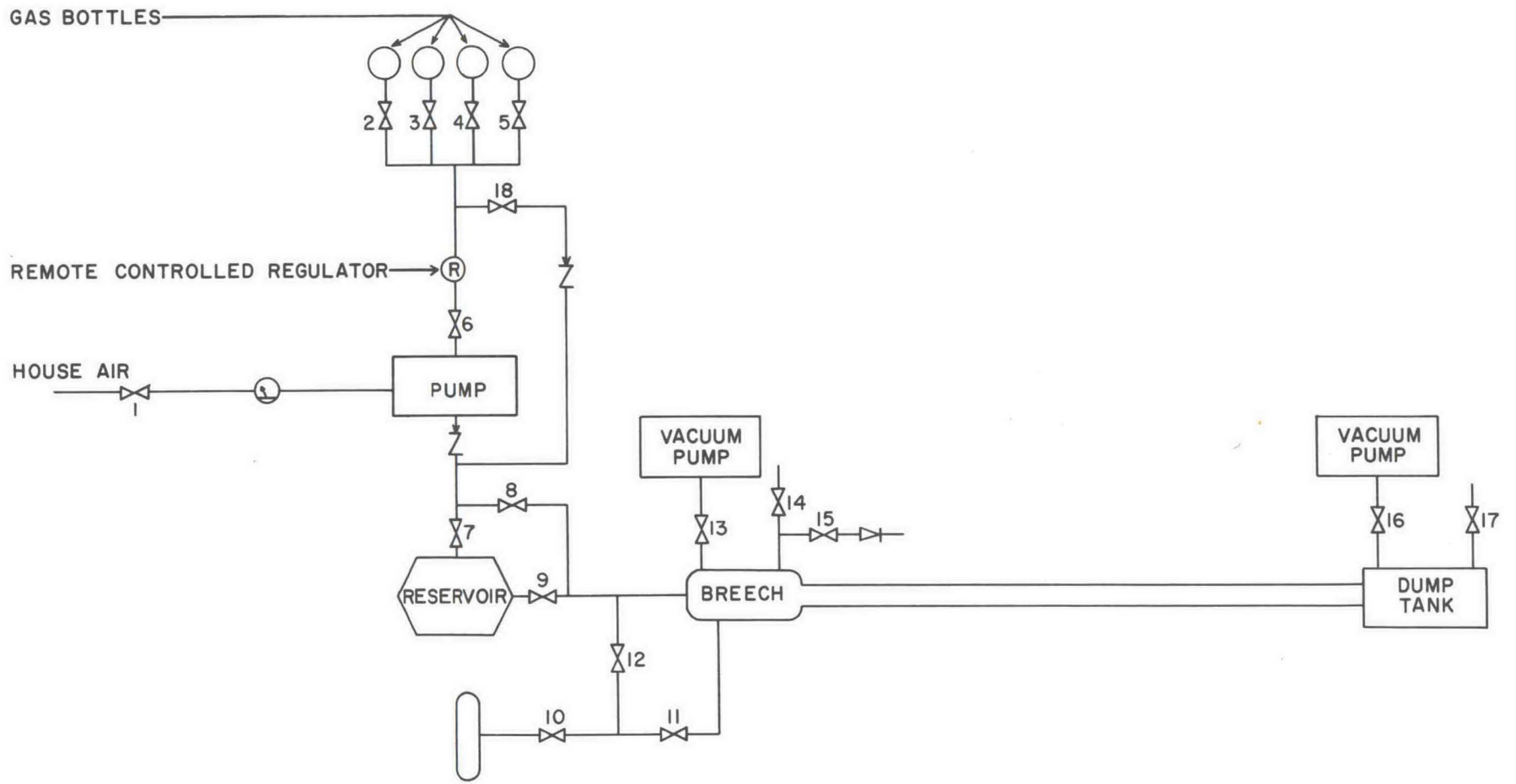


Fig. 13. Gas flow circuit.

In the event that pumping is necessary the operator may route the high pressure gas to a one cubic foot storage reservoir for later use, or pump directly into the breech reservoir.

It is normal procedure to fill the breech reservoir fifty to one hundred psi above the desired shooting pressure and then allow the gas pressure to stabilize at ambient temperature. This makes it necessary to have some means of slowly relieving the breech pressure to the desired pressure.

A normally open high pressure valve with a restricted orifice open to the atmosphere is used to facilitate bleeding the breech pressure to the desired value. This valve (No. 15) is in parallel with the breech fill line. One other valve (No. 14) with a full orifice open to the atmosphere and also in parallel with the breech fill line is of the normally closed configuration and is used for "dumping" the pressure in the breech to the surroundings should an emergency arise.

To facilitate the use of both breeches without having to make extensive changes in the system, valves number 10 and 12 (Fig. 13) were incorporated into the system. Valve No. 11 always remains the firing valve, so as not to present any chance of confusion on the part of the operator. Valves No. 10 and 12 are on the same circuit and are operated in such a way that only one may be open at any time. In effect these two valves afford the possibility of operating both breeches from essentially the same system. By opening valve 10, valve 12 is simultaneously closed and the system is ready to accept the double diaphragm breech. In the other mode (valve 12 open, valve 10 closed) the system is used to operate the wrap-around breech.

2. Control Panel

The control panel (Fig. 14) is divided into two sections. One affords the control of operations and the other enables the operator to monitor the influence of the controlling action taken.

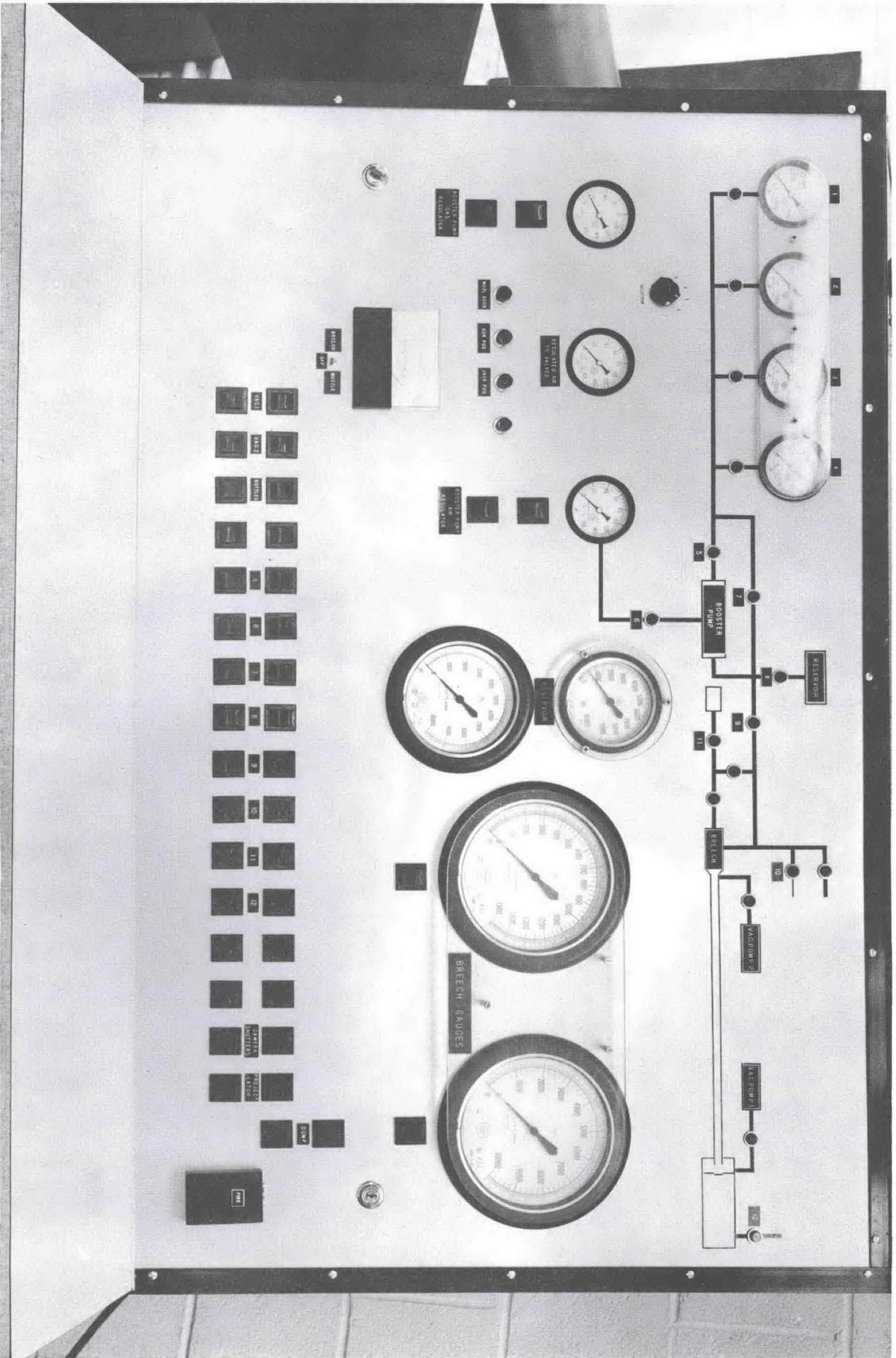


Fig. 14. Control panel.

The control section consists of a double row of illuminated pushbuttons across the lower extremity of the panel face. The upper row is green and the lower red. These pushbuttons control all valves, both vacuum pumps, the projectile latch and the oscilloscope camera shutters. The circuits are designed in such a way that all lights must be green immediately prior to firing. This feature enables the operator to make one final check just prior to firing to be sure the system is "go". There is one set of pushbuttons which are not in-line with the others. These buttons are at the right end of the row. The upper button, which is the one out of sequence, is the "dump" actuating button. Upon depressing this pushbutton the previously mentioned dump valve is actuated and all other valve circuits are simultaneously opened, thereby causing all other valves to close.

The center section of the panel contains the pressure monitoring devices. At left, the $2\frac{1}{2}$ " diameter gauge reads the pressure of the bottle gas entering the high pressure pump. Directly below this gauge are two pushbuttons which actuate a motor-driven pressure regulator, thus allowing for remote control of the pump inlet pressure. The vent gauge in this sequence indicates the air pressure to the high pressure valve actuators. The third gauge reads the air inlet pressure to the pump. The two buttons below this gauge enable one to regulate the air inlet pressure to the pump.

The gauge directly in the center of the panel monitors the reservoir pressure. Below this gauge a thermo-couple gauge readout indicates the pressure in the barrel when under a vacuum.

Breech pressure is monitored by the two large gauges on the right. Both gauges read to an accuracy of $\pm\frac{1}{4}\%$ of full scale. The left gauge is calibrated in 5 psi subdivisions and indicates pressures from 0 to 1500 psi. The right gauge is calibrated in 25 psi subdivisions and indicates pressures from 0 to 10,000 psi. These gauges are connected to the breech fill line by capillary tubing (1/8" OD x 0.028" wall 316 SS). The low pressure gauge may be

remotely switched into or out of the breech pressure line. If the low pressure gauge is inadvertently left in the system above 1500 psi, a burst diaphragm will rupture and a surge check valve will close, thereby isolating it from the system.

Visible on the upper portion of the control panel is a schematic representation of the high pressure piping system. Each valve in the system and its location with respect to the high pressure flow is denoted on the schematic by a numbered, red indicator light. The corresponding number is found between the two rows of pushbuttons. This feature reduces the possibility of actuating a critical valve at an inopportune time.

The electrical control circuit is shown schematically in Appendix A. Appendix B is a parts list showing the principal parts used.

IV. INSTRUMENTATION AND ANCILLARY EQUIPMENT

In addition to the gun and control system, electronic instruments were either purchased or built to serve as recording devices. The principal instrumentation consists of ten oscilloscopes. These include six Tektronix type 581/585, two Tektronix type 454, one Tektronix type 519, and one Tektronix type 555. These scopes provide eleven recording channels with a frequency response adequate for use with essentially all currently feasible measurement techniques.

The scopes are supplemented by a 100 MHz time-interval counter, Hewlet-Packard type 5275A with crystal controlled oscillator, and a pulse generator, E-H Co. Model 120D. These are used principally for timing devices.

A number of electronic devices have been constructed by students to serve special purposes. These include timing and tilt pulse-shaping circuits, a quartz-gauge calibration device, and a manganin-gauge power supply. These devices are described in detail below.

In addition to electronic instruments other major auxiliary equipment includes a lapping machine, a toolmaker's microscope (which serves for measuring traces on films and other purposes) and a diamond cut-off saw.

A. Velocity and Tilt Circuits

The projectile velocity is measured electronically immediately before the target is impacted when the grounded projectile shorts four pins of accurately known separation. The projectile tilt at impact is measured by four pins in the plane of the target which are shorted by the impacting face of the projectile.

Both the velocity and tilt circuits are identical in design and operation. The circuit for each consists of four triggerable constant current sources connected to a load resistor as shown in Figure 15. The trigger inputs for these constant current sources are the velocity pins for the velocity circuit and the tilt pins for the tilt circuit.

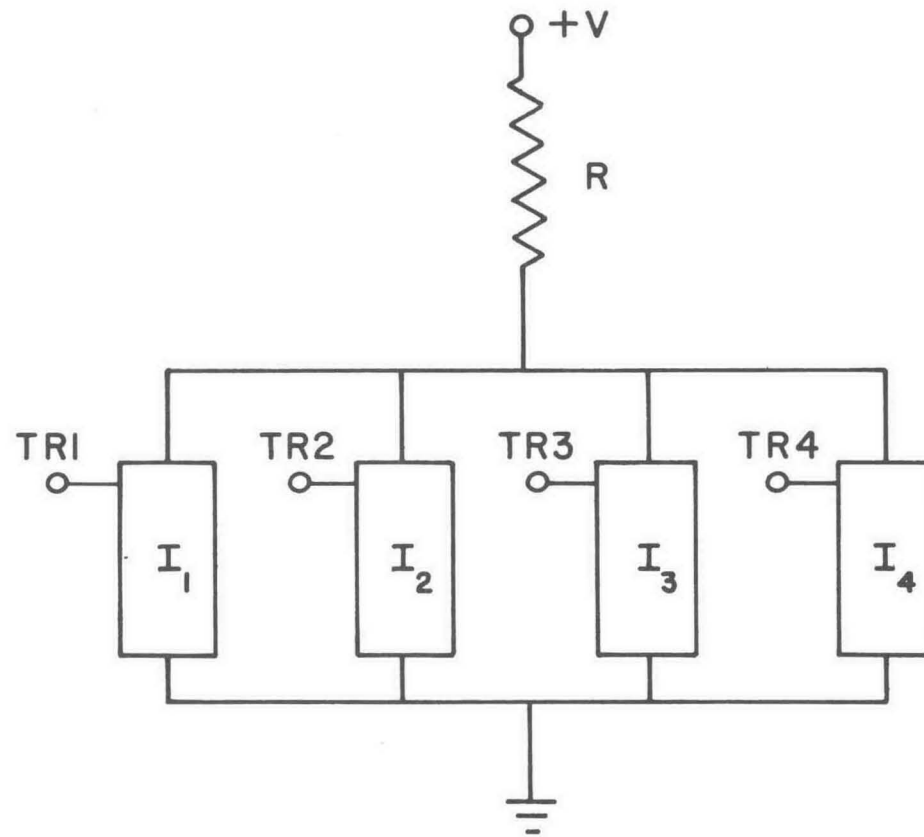
Once triggered these constant current sources remain on until reset manually by the operator. This feature prevents any one of the current sources from turning on and then off due to a loss in the ground connection at the pin input. Thus, the voltage across the load resistor is given by:

$$V(t) = R(I_1H(t-t_1) + I_2H(t-t_2) + I_3H(t-t_3) + I_4H(t-t_4)), \quad (1)$$

where

$$\begin{aligned} H(\xi) &= 0, & \xi < 0, \\ H(\xi) &= 1, & \xi \geq 0, \end{aligned}$$

and t_1 , t_2 , t_3 , and t_4 correspond to the times at which pins 1, 2, 3 and 4 for either the tilt or the velocity circuit are grounded by the projectile. Further, the current ratios $I_1::I_2::I_3::I_4$ determine the relative voltages across the load resistor R for the respective pin shortings 1, 2, 3, and 4. In the case of the velocity circuit the ratios are all 1:1 so



TR1, TR2, TR3, TR4 – TRIGGER INPUTS

Fig. 15. Operational schematic of velocity and tilt circuits.

that the voltage steps are equal for all pin shortings. Figure 16 shows an oscilloscope voltage-time record for a typical velocity measurement.

For the tilt circuit the current ratios have been set at 1::2::4::8 for the circuit inputs 1, 2, 3, and 4 respectively. These ratios were chosen so that the sequence of pin closures can be discerned in the case of simultaneous pin shortings, i. e. any additive combination of 1, 2, 4, or 8 will correspond to a unique voltage combination on the measurement oscilloscope.

The tilt and velocity circuits do not have infinite rise-times as implied by Eq. (1). In fact, the combined rise-time of either circuit and a Type 585A Tektronix oscilloscope normally used for the measurement is typically 10 nanoseconds for any pin closure. A typical tilt record is shown in Fig. 17.

Figure 18 is a block schematic of both the velocity and tilt circuits. When the input pins are all ungrounded the circuit may be placed in a "reset" mode by depressing the reset key. Any subsequent input pin shorting will change the circuit from the reset mode to the "set" mode. To the operator these two modes are distinguishable by the use of an indicator lamp, which is turned on when the circuit is in the reset mode. (See Figure 18).

Describing the reset mode more specifically in terms of circuit operation, each pin input is clamped on electrically by means of a 220 ohm resistor connected to the 3.6 volt supply at the input of "nor" gates G1, G2, G3, and G4. The "nor" designation means that the sign of the output of the gate is opposite to the input. The outputs of nor gates G1, G2, G3, and G4 are connected to the "set" terminals of gates I1, I2, I3 and I4 respectively. I1, I2, I3 and I4 are properly designated as set-reset flip-flops. It is the property of these gates that produces the set and reset modes in the circuit.

A set-reset flip-flop is a bistable electronic device. A positive going pulse of amplitude greater than 0.7 volts applied to the reset input will place the flip-flop in reset state where it will remain until a

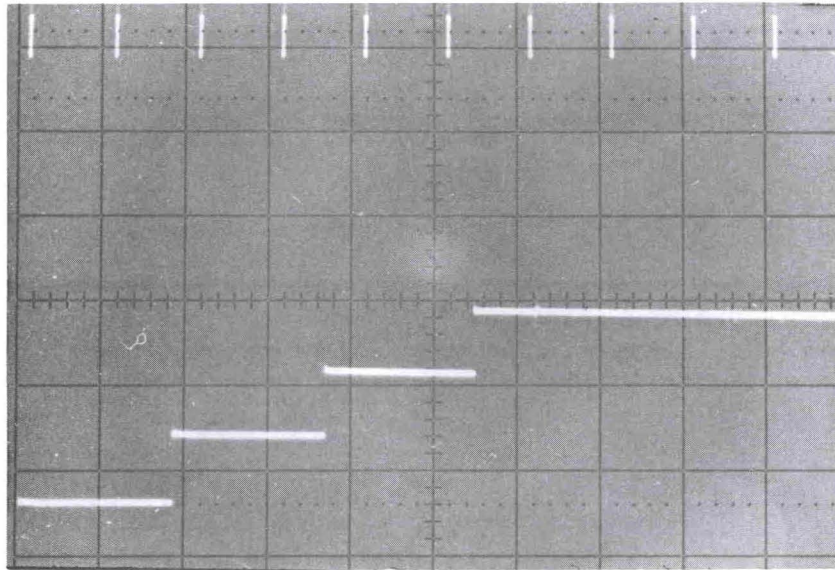


Fig. 16. Typical record for projectile velocity measurement.

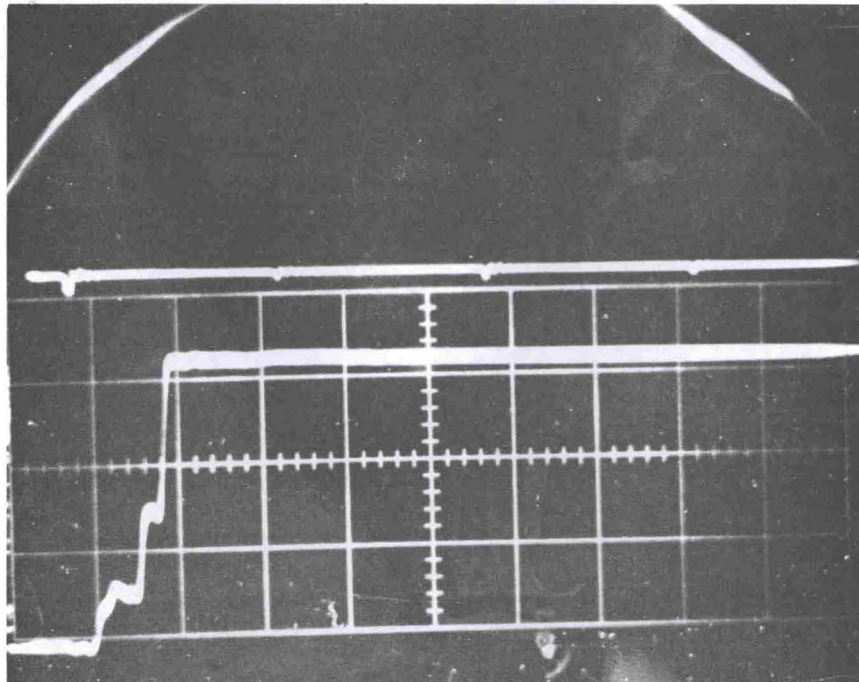


Fig. 17. Typical record for measuring tilt of impacting surfaces.

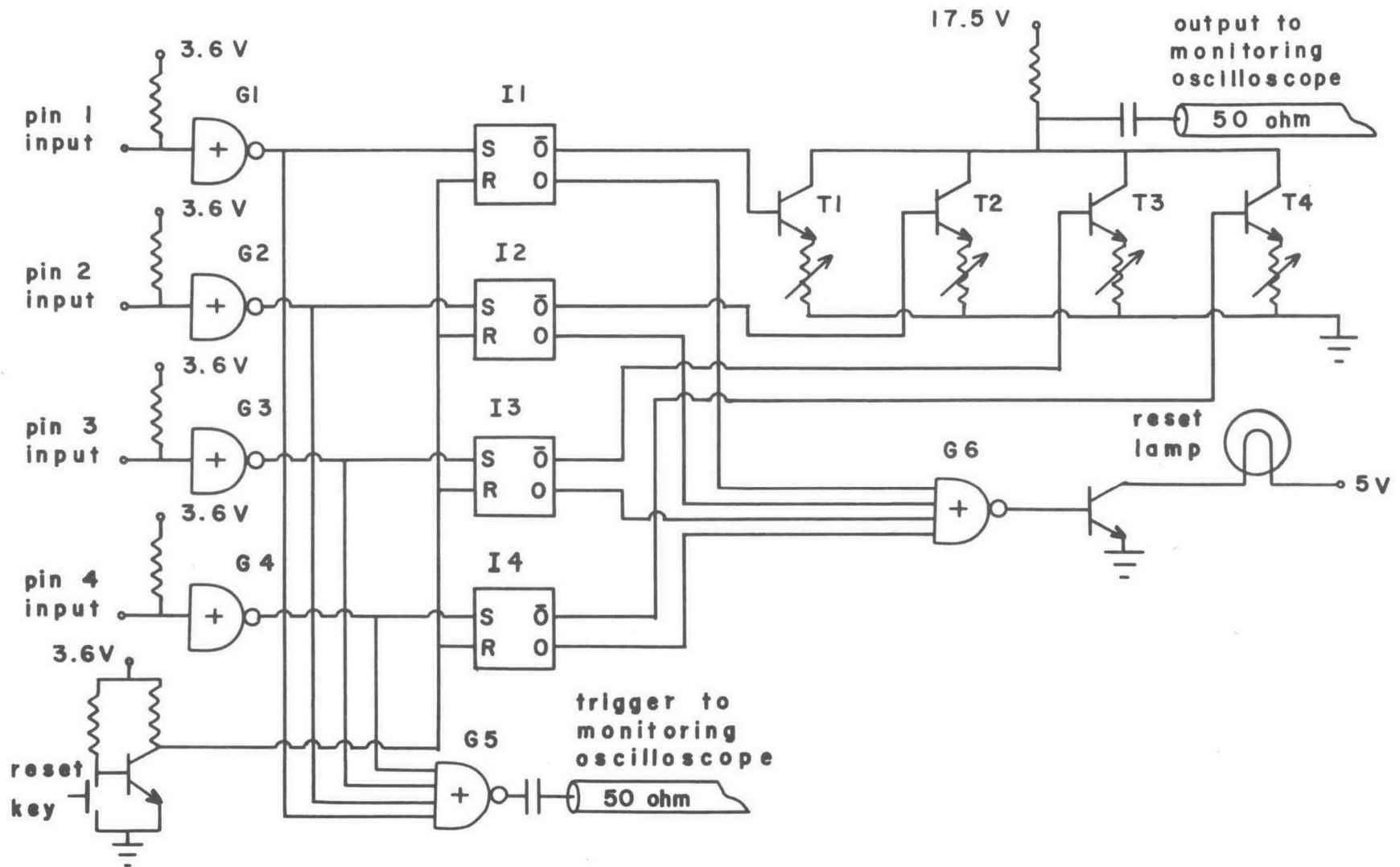


Fig. 18. Block schematic of velocity and tilt circuits.

positive pulse is applied to the set input. When a pulse is applied to the set input the device flips to the set state and remains there until again reset. The device has two outputs that will be designated here as "O" and " \overline{O} ".

When the reset key in the circuit is depressed a positive pulse from transistor T5 connected to the reset inputs of I1, I2, I3 and I4 places the circuit in the reset mode. The "O" output of each flip-flop is fed into G6, and a four input nor gate, the output of which turns on a transistor to drive the reset lamp.

The " \overline{O} " outputs of the set-reset flip-flops I1, I2, I3 and I4 are connected to the base junctions of transistors T1, T2, T3 and T4 respectively. These transistors are then turned on when the circuit is in the reset mode. Each transistor acts as a current source and is connected to resistor R1 which sums the current from these four transistors. The variable resistor attached to the emitter of each transistor is used to adjust the current flowing through each transistor in order to provide the desired current ratios as previously mentioned.

The transistors T1, T2, T3 and T4 then act as switches, either permitting or preventing the flow of current through resistor R1. These switches are all open when the circuit is in the reset mode since all transistors will be held on by the " \overline{O} " outputs of gates I1, I2, I3 and I4. The voltage at point A in the circuit as shown in Figure 18 will be for the reset mode:

$$V_o = 17.5 - 100(I_1 + I_2 + I_3 + I_4). \quad (2)$$

Now consider shorting input 1 of the circuit to ground. The voltage output of G1 will rise from 0 to 3.6 volts. This positive pulse at the output of G1 flips I1 to the set position which turns off the reset lamp and turns off transistor T1. The voltage at point A will now be given by:

$$V_1 = 17.5 - 100(I_2 + I_3 + I_4). \quad (3)$$

The voltage change at A appears as a step on the oscilloscope proportional to I_1 , i. e.,

$$V_1 - V_0 = 100 I_1.$$

When input 1 is shorted to ground the positive pulse from the output of G1 also provides an input to G5 -- a four input nor gate. This gate produces a negative-going pulse which is used to trigger the monitoring oscilloscope.

Channels 2, 3 and 4 all operate in the same manner as described above for channel 1. The complete circuit diagram for the velocity and tilt circuits is shown in Figure 19.

The velocity circuit has one feature absent in the tilt circuit. Attached to each of channels 3 and 4 of the velocity circuit is a signal output circuit as shown in Fig. 19. When pin 3 or pin 4 is shorted, a negative pulse will appear at the respective auxiliary outputs. These outputs may be used to trigger external circuitry, i. e. manganin gauge current supplies, time interval counters, measurement oscilloscopes, etc.

B. Quartz Gauge Calibration Circuit

The quartz gauge technique is used to measure pressure profiles during shock compression. Based upon the piezoelectric properties of quartz, this gauge produces a current that is proportional to the pressure difference across the thickness of the quartz⁹. For pressures below 30 kilobars the current-pressure relation is accurately known and for a given current observed from the gauge the pressure may be computed. Consequently, it is desirable to calibrate the measurement oscilloscopes directly to establish an accurate relation between the scope deflection and the current output from the quartz gauge. A calibration circuit has therefore been developed to feed a pulse of known current amplitude through the instrumentation cable and to the oscilloscopes that are to monitor the output from the gauge.

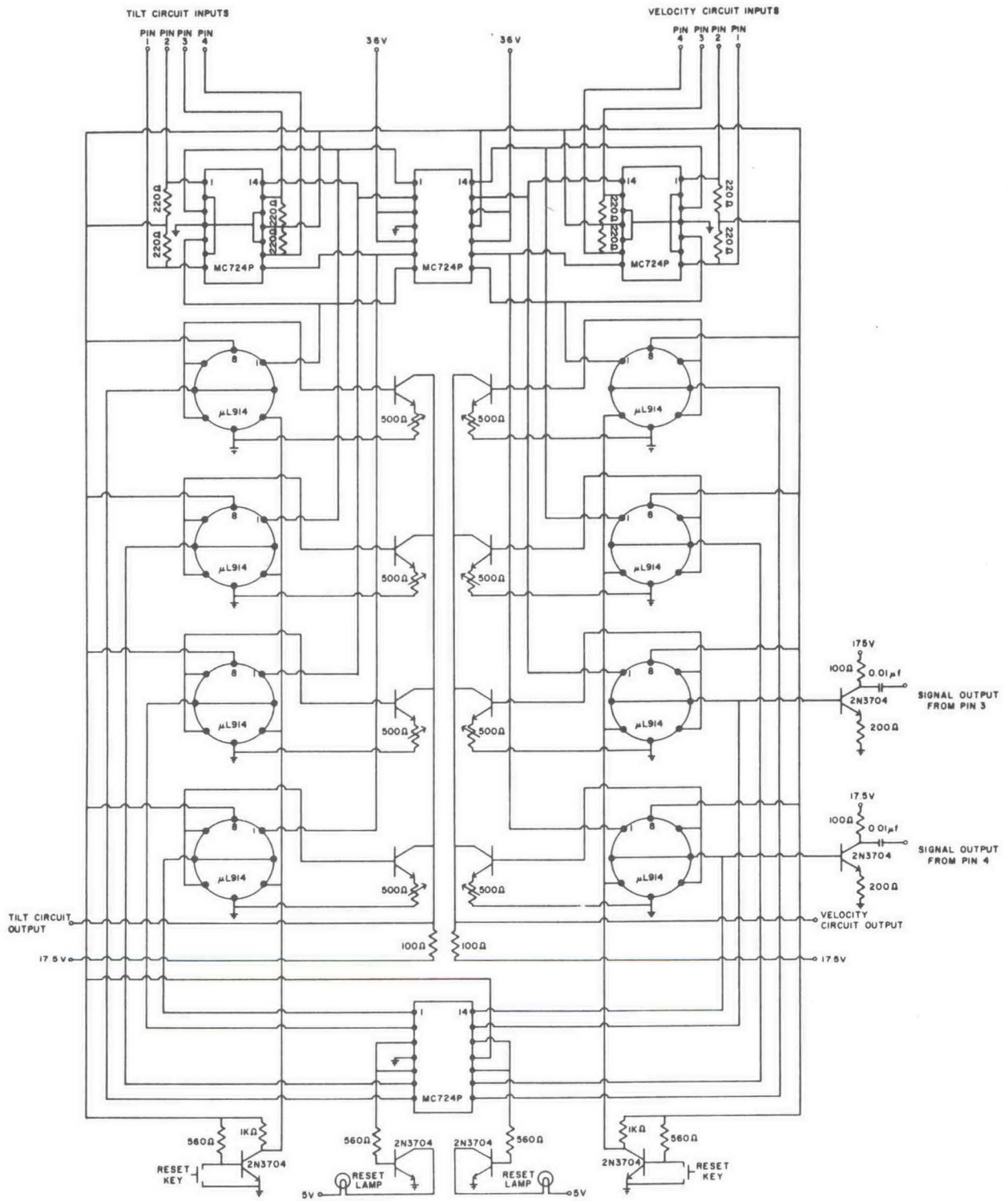


Fig. 19. Circuit diagram for velocity and tilt circuit.

The quartz gauge calibration circuit consists mainly of a unijunction pulse generator, a monostable multivibrator, and two switching transistors. Referring to the circuit diagram of Figure 20, a unijunction transistor U1 pulses a monostable multi-vibrator I1 with a repetition rate of approximately 1 KHz. With each pulse from U1, I1 turns on and remains on for about 5 micro-seconds. Initially when I1 is off current flows from point A in the circuit through transistor T1 to the negative supply voltage. As I1 turns on the current is switched to flow through transistor T2. This sends a current pulse down the instrumentation cable that is to be used in monitoring the quartz gauge output. The current before switching is measured accurately by the use of a precision digital ammeter. Therefore, the magnitude of the voltage step produced on the oscilloscope is related to an accurately known current value, since the inductor time-constant is large compared to the five microsecond time interval of the switched current pulse. The magnitude of the current step may be varied from 80 ma to 300 ma by varying the supply voltage from 4 to 15 volts.

C. Manganin Gauge Pressure Transducer

The manganin gauge pressure transducer is a useful device at pressures in excess of those observable by quartz gauges or if the validity of the calculation necessary to eliminate the error due to impedance mismatch at the specimen-quartz interface is in doubt.¹⁰ Auxiliary equipment needed for the manganin gauge technique consists of a constant current supply, an adequate gauge and mounting facility, and proper recording oscilloscopes and cables.

1. Constant Current Supply*

The present supply utilizes an inductor as the essential component in maintaining constant current during the recording time of the gauge. The operating characteristics can be understood with

* To be published in Rev. Sci. Instr.

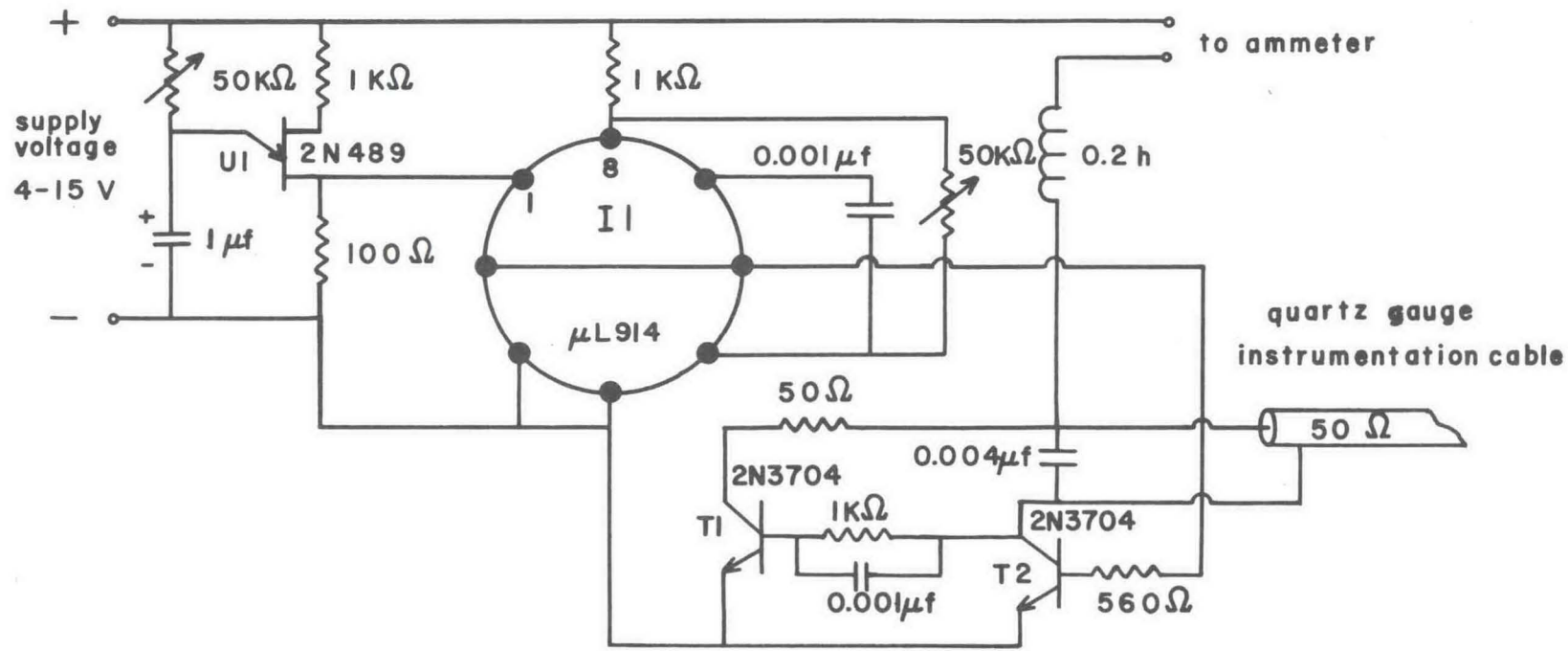


Fig. 20. Diagram of quartz calibration circuit.

the aid of the block diagram in Fig. 21. Briefly, in the standby state a transistor gate is held open, maintaining a current in the inductor. Prior to arrival of the stress wave at the gauge the supply is triggered externally. The electronic switch opens a silicon control rectifier and closes the transistor gate, rerouting the current through the gauge.

A schematic of a working constant current supply is shown in Fig. 22. Normal operating voltage and current is 50 volts and 0.5 amperes. This is supplied by a stable (less than 0.1% fluctuation) floating voltage source.

The constant current supply completes an operational cycle in the following manner. Upon closing switch S1, the potential on the anode of SC1 comes to 50 volts. This turns on transistors T2 and T1 respectively. In this standby state current follows the path from the supply through inductor I1, transistor T1, and then returns. The base current for transistor T2 which must traverse the gauge element is less than one milliamp and hence constitutes no heating danger to the gauge element. To switch the supply to the active state, a positive pulse is injected at the trigger input. This trips SC2, discharging capacitor C1 across transformer TF1. This ramp pulse is coupled through TF1 and trips SC1. The potential across SC1 drops to zero. This turns off transistors T2 and T1. The current is then rerouted through the gauge and SC1. After approximately fifty microseconds, the variable delay consisting of the UN914 trips SC4. The pulse is coupled through TF3, which in turn trips SC5. The opening of SC5 relieves the gauge of the current. This protects the gauge from overheating while pulsing the supply during preliminary setup. Previously, when SC2 tripped, the pulse was also coupled through transformer TF2 and tripped SC3. The discharge of capacitor C2 through the coil of relay R1 eventually mechanically breaks the current circuit and allows SC1 and SC5 to reset. The time for this to occur is approximately two milliseconds. The high back-emf inevitably produced by the inductor when the circuit is broken is limited by the ignition of a neon

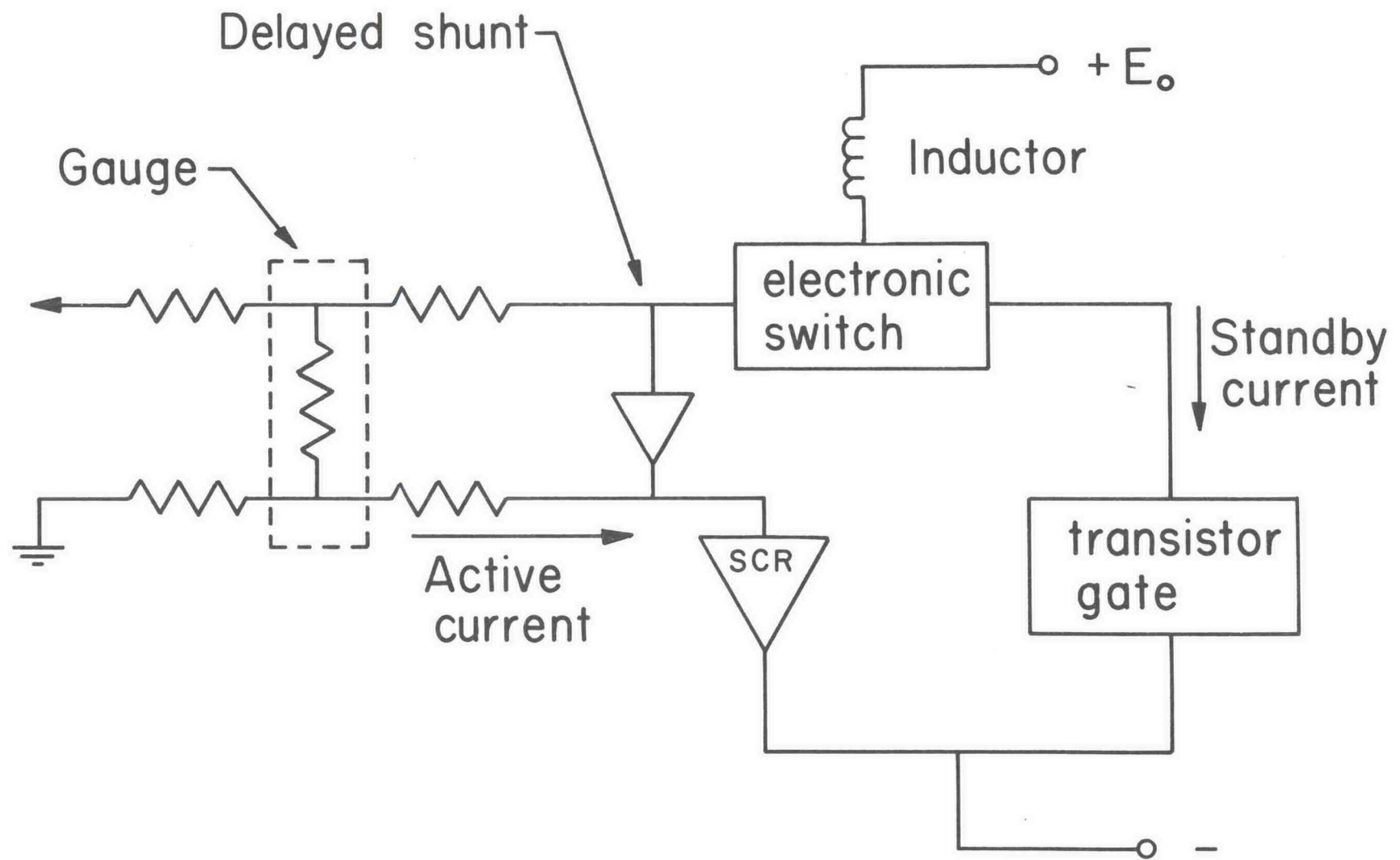


Fig. 21. Block diagram of constant current supply for use with manganin gauges.

bulb across the circuit. The supply has now completed a cycle and has returned to the standby state.

2. Gauge Construction

Gauges used are of the four terminal type, shown in Fig. 23. They are produced by a photoetch technique and are initially attached to a plastic film.¹¹ The gauges are easily removed from the film by immersion in boiling acetone. The sensitive element spans less than a 0.125" square while the gauge depth is approximately 0.0008 inches. The aspect ratio (width/depth) is about 5 for the wire in the sensitive element. The resistance of the sensitive element is two ohms while that of the terminal leads is about one ohm.

In target construction, the gauge is mounted directly between two slabs of the material under observation if that material is a nonconductor. If not, the gauge is insulated from the material by a 0.00035 inch mylar film. The bonding is effected by air-evacuated epoxy. The dimension of the sandwich in the latter case is approximately 0.002 inches. Since the shock wave transit time of this sandwich is on the order of ten nanoseconds and since in general there is a sample-epoxy impedance mismatch, fidelity of the wave profile will deteriorate to an extent depending on the magnitude of the mismatch. In non-conducting materials this risetime effect has not been noticed. Stress profiles at the 35 kb level in CdS have been observed by both the quartz gauge and manganin gauge technique. Allowing for the impedance-mismatch with quartz they were found to be closely comparable. In constructions involving both conducting and nonconducting samples, the gauge terminal leads were brought out the sides of the sample. This allowed recording times of from two to five microseconds before the gauge leads were either severed or shorted, disrupting the current flow. This recording time is sufficient for most applications. Figure 24 shows a representative recording obtained with this system.

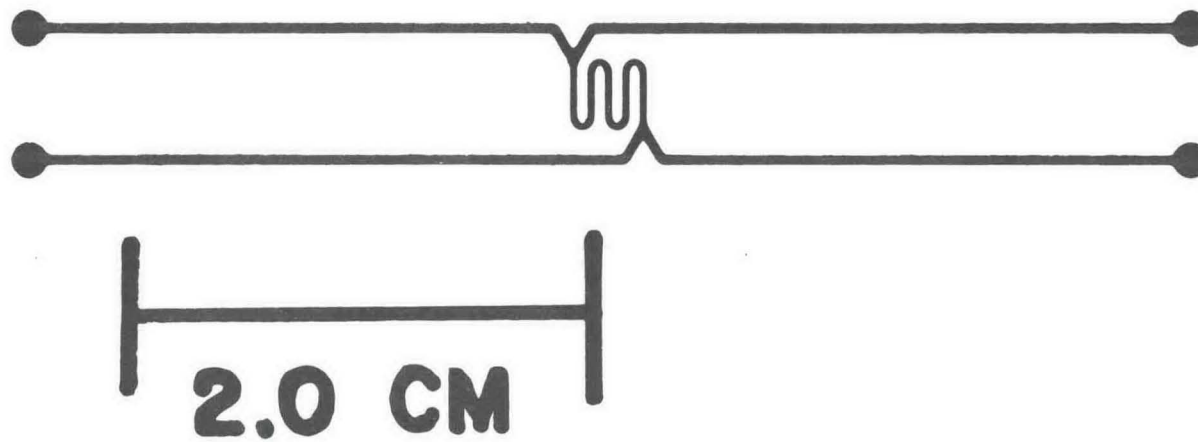


Fig. 23. Manganin grid for use as in-material gauge.

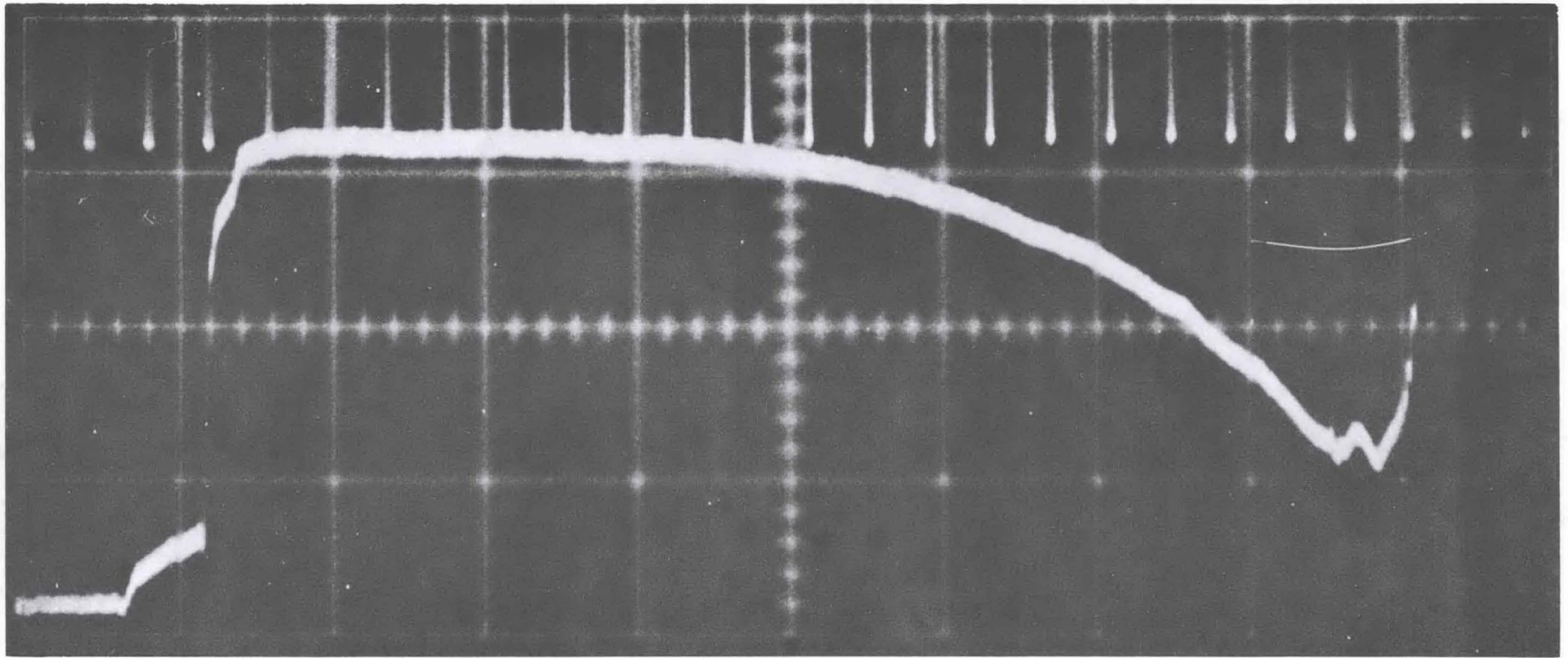


Fig. 24. Voltage-time record of a 38 kilobar final state shock wave in 6061-T6 aluminum utilizing a manganin gauge. The scale is 0.5 μ sec/div.

3. Recording Facility

The voltage time profile is recorded on a 585 Tektronix oscilloscope with the aid of a type 1A5 offset pre-amplifier plug-in unit. This unit allows observation of the profile which is superimposed on top of the voltage step developed across the gauge when the constant current supply is initially turned on. This voltage step, knowledge of which is necessary for data reduction, is measured during the preliminary setup. This measurement is performed using the comparison voltage available on the 1A5 plug-in unit in conjunction with a precision voltmeter. The comparison voltage is used to nullify the voltage step while the comparison voltage is in turn monitored by the voltmeter. This measurement can be made to well within 0.5% accuracy.

Cable termination is carried out at the gauge rather than the oscilloscope end of the line. Figure 25 shows a schematic gauge with representative termination resistors. Termination at the gauge rather than at the oscilloscope eliminates the problem of a current shunting the gauge and therefore simplifies data reduction. In practice the gauge element will change resistance by about an ohm as the stress profile passes the gauge. The terminating resistance values should be selected so that proper termination is effected when the gauge resistance is in its final state.

V. GUN PERFORMANCE

A. Projectile Velocity

Predicted velocity curves for the gun as designed using nitrogen or helium are shown in Fig. 26. Also shown are representative data points derived from the approximately fifty shots fired to date at pressures up to 3000 psi. The agreement is seen to be good for helium, but is less satisfactory for nitrogen. The reason for the discrepancy is not established; possibly throttling at the orifices connecting the breech to the barrel, which is more important for nitrogen than for

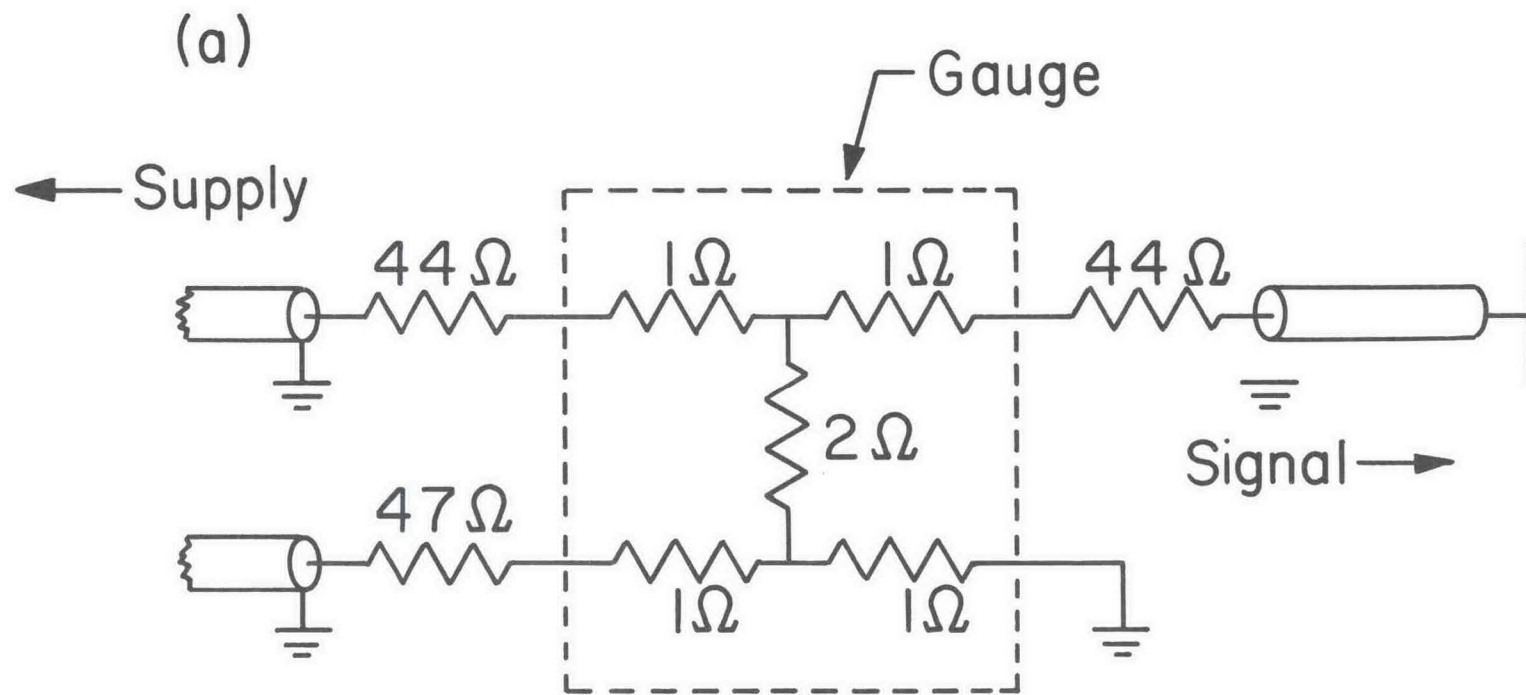
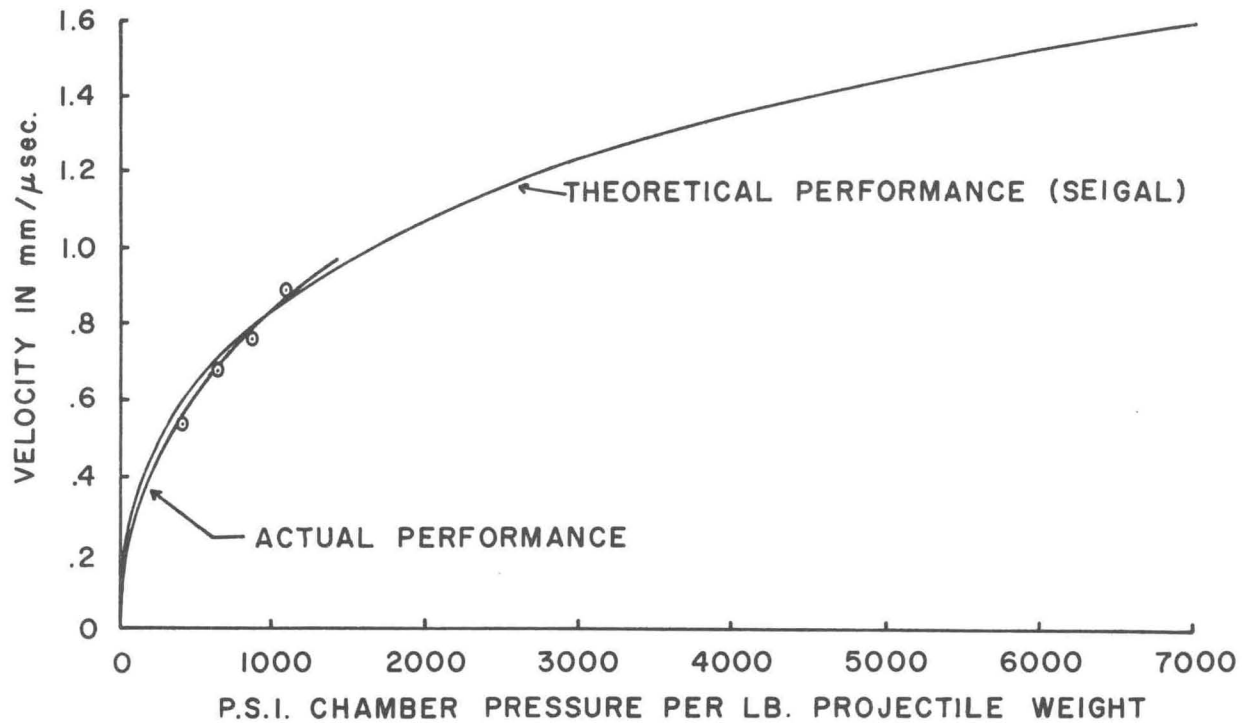
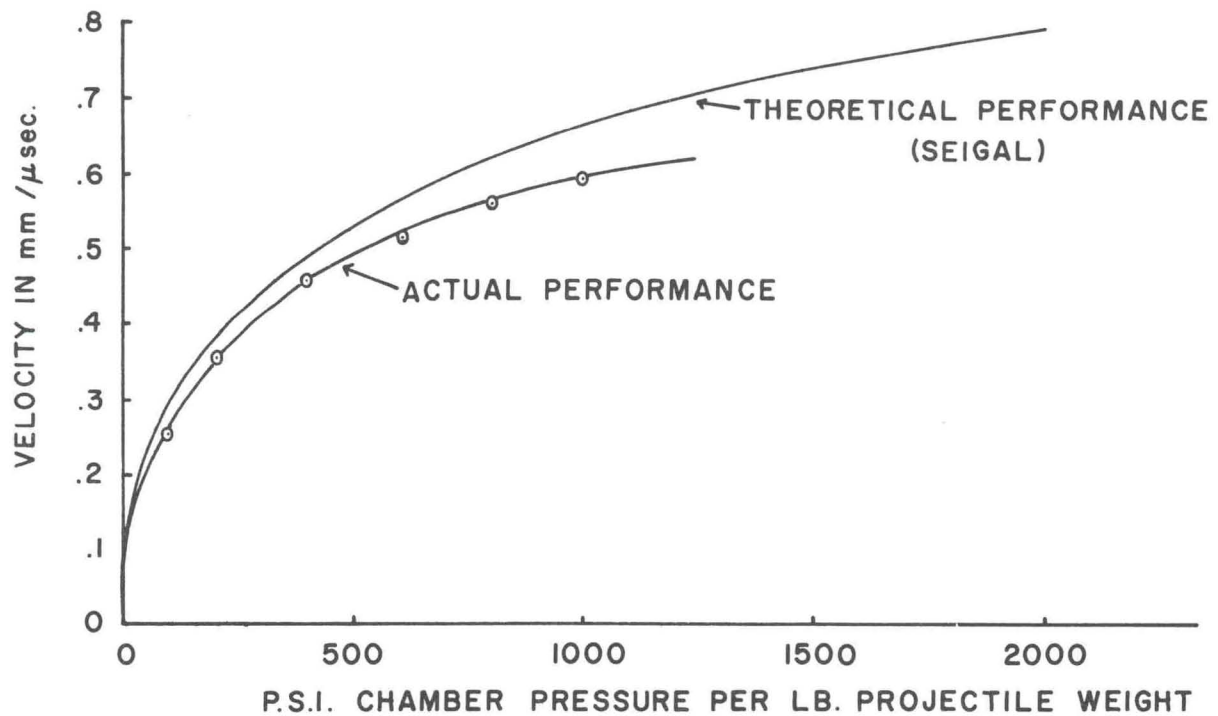


Fig. 25. Manganin gauge equivalent circuit including representative gauge and terminating resistor values.



GUN PERFORMANCE WITH HELIUM DRIVER GAS



GUN PERFORMANCE WITH NITROGEN DRIVER GAS

Fig. 26. Measured projectile velocities compared with theoretically predicted curves.

helium, is the source of the difference. The reproducibility is very good, amounting to about $\pm 1\%$ at velocities above $0.2 \text{ mm}/\mu\text{s}$.

B. Tilt

The major question with regard to this design is whether or not adequate control of the tilt of the projectile face with respect to the target face can be maintained. In order not to seriously degrade the time resolution of the recording instrumentation it is desirable that the closure time of the two surfaces (of four-inch diameter) be less than about 50 ns. The time required for the induced stress wave to sweep past a gauge whose lateral dimensions in a plane parallel to the impact surface is 10 mm or less will then be no more than 5 ns. This time is comparable to the response time of the oscilloscopes in use (85 MHz frequency response).

The geometrical tilt required is thus a function of projectile velocity and varies between 0.2 milliradian at a projectile velocity, v , of $0.1 \text{ mm}/\mu\text{s}$ to 2.0 milliradian at $v = 1.0 \text{ mm}/\mu\text{s}$.

Our experience to date shows that, with a few exceptions probably attributable to errors in initial alignment or to faulty target construction, the tilts achieved are frequently 0.1 to 0.2 milliradian and are consistently below 0.5 milliradian. This degree of tilt could arise solely from the allowed clearance ($3 \text{ to } 3.5 \times 10^{-3}$ inch) between the projectile and the barrel. Thus the tilt is adequate for most experiments and, where it is demanded by an unusual experiment, improvements in tilt can probably be achieved with tighter fitting or longer projectiles.

VI. RESEARCH PROGRAM

Several research problems are currently underway, simultaneously with the development of recording techniques. The quartz technique⁹ is reasonably well established in the laboratory and manganin gauges¹⁰ are beginning to be used. As confidence is developed in the use of these techniques

effort will be directed toward the use of electromagnetic velocity gauges¹² and laser interferometry.¹³ Some preliminary studies of the latter methods have already been made.

The research problems fall into two major categories -- phase transitions and constitutive relations. The work on phase changes is directed to the study of some heretofore poorly understood transitions, and to the development of the mixture technique reported by Dremmin¹⁴ for minimizing stress anisotropy. Particular interest is in the kinetics of these solid-solid transitions.

The study of constitutive relations is directed toward an improved understanding of dynamic yielding in single crystals of measurable dislocation densities.

The individual research problems currently under investigation are outlined below.

A. Cadmium Sulfide (CdS)

CdS is known to undergo a phase transformation at a static pressure of 27 kbar.¹⁵ This transformation from a wurtzite to a rocksalt structure is accompanied by a 19% change in specific volume. Kennedy and Benedick¹⁶ report this transition under shock loading conditions at 31.5 kbar and 28 kbar respectively in single crystals shock-loaded parallel to the c-crystal axis and perpendicular to it. They base their findings on an observed double wave structure and on the calculated change in specific volume. However, the elastic waves in CdS single crystals (42 kbar for the c-axis and 21 kbar perpendicular to it) will themselves give rise to a double wave structure. There is thus some uncertainty whether the observed two-wave structure is due to the phase change.

The purpose of the present work is to reduce the elastic limit essentially to zero so that shock experiments will yield essentially hydrostatic pressure-volume data. A technique similar to that employed by

Dremin and Karpukhin is being used.¹⁴ Lucite, which has a well-known Hugoniot, is mixed with CdS powder and formed into sample specimens. Shock experiments on the mixture then yield pressure-density data which can be reduced to give corresponding values of pressure and density in the CdS. These data then allow for calculation of both shock and particle velocities in the CdS and hence the determination of its Hugoniot.

Two preliminary shots, one using a quartz gauge and one using a manganin gauge, have been fired. These data tentatively suggest a phase transformation between 25 and 28 kbar.

B. Lithium Fluoride (LiF)

Eight experiments have been performed with lithium fluoride single crystals oriented in the (100) direction. Of these, three corresponded to driving stresses in the 11-14 kbar range and five represented driving stresses of about 25 kbars. In all of the shots quartz gauges were used to determine stress states in the samples. The objective of this series of shots was to study the behavior of the elastic precursor decay in comparison to existing theoretical predictions of decay for a stress relaxing solid (for example, see references 17-19). Lithium fluoride is an ideal material to study in this respect since an abundant amount of work relating yielding mechanisms to mechanical properties²⁰ has previously been performed on it by other investigators.

The crystals studied were purchased from Semi-Elements, Inc. as optical quality LiF. The purity of the material was about 99.99% LiF and the mosaic spread within subgrains was less than 2° . Since the dislocation density is important to theoretical predictions of precursor decay, it was measured for most of the crystals that were shot. The nominal overall dislocation density was about 2×10^6 for each sample, although in some of the samples there were areas which exhibited major fluctuations from this value. Also, it was found that the static yield strength in uni-axial compression ranged from about 0.15 kbars to 0.3 kbars.

For the series of shots at 25 kbar driving stresses, it was observed that the elastic wave amplitudes for a given propagation distance were somewhat inconsistent from sample to sample. This effect is illustrated in Fig. 27 where two different specimens, each about 2 mm thick, were impacted with an aluminum projectile. Although these two samples appeared to be approximately in the same initial state with respect to dislocation densities and chemical purities, there is a significant difference in elastic precursor amplitude and structure in the two cases. In addition, it was found that high-temperature annealing did not appreciably affect the structure of the profiles shown in Fig. 27.

Another point illustrated in the figure is that the overall profile of the wave corresponding to the higher Hugoniot elastic limit is more spread out than in the other. This spreading behavior has been observed on all of the specimens tested and, in general, increases with increasing sample thickness. The magnitude of the effect appears to be a function of elastic precursor amplitude, as illustrated in the figure.

The way the profile changes with propagation distance is further illustrated in Fig. 28. This profile was obtained from a sample about 15 mm thick. The rise time of the plastic wave for this sample is about 4 times that for the thinner specimens. This suggests that the profile may not be steady, even for large propagation distances. Another important point illustrated in the figure is the transitional behavior of the wave shape between the elastic and plastic waves, indicating a third wave. Since static equation of state work does not indicate a volume transition in LiF for the stress levels studied here, the cause of the transitional behavior in the waveform is not presently understood.

The primary objective of future experimental work in lithium fluoride will be to isolate the causes for the lack of reproducibility observed in the present work and to establish a precursor decay curve for lithium fluoride in an initially known state. Secondly, we will study the profile of the plastic wave in more detail, with an emphasis on the conditions under which the profile becomes steady and how it changes with different driving stresses.

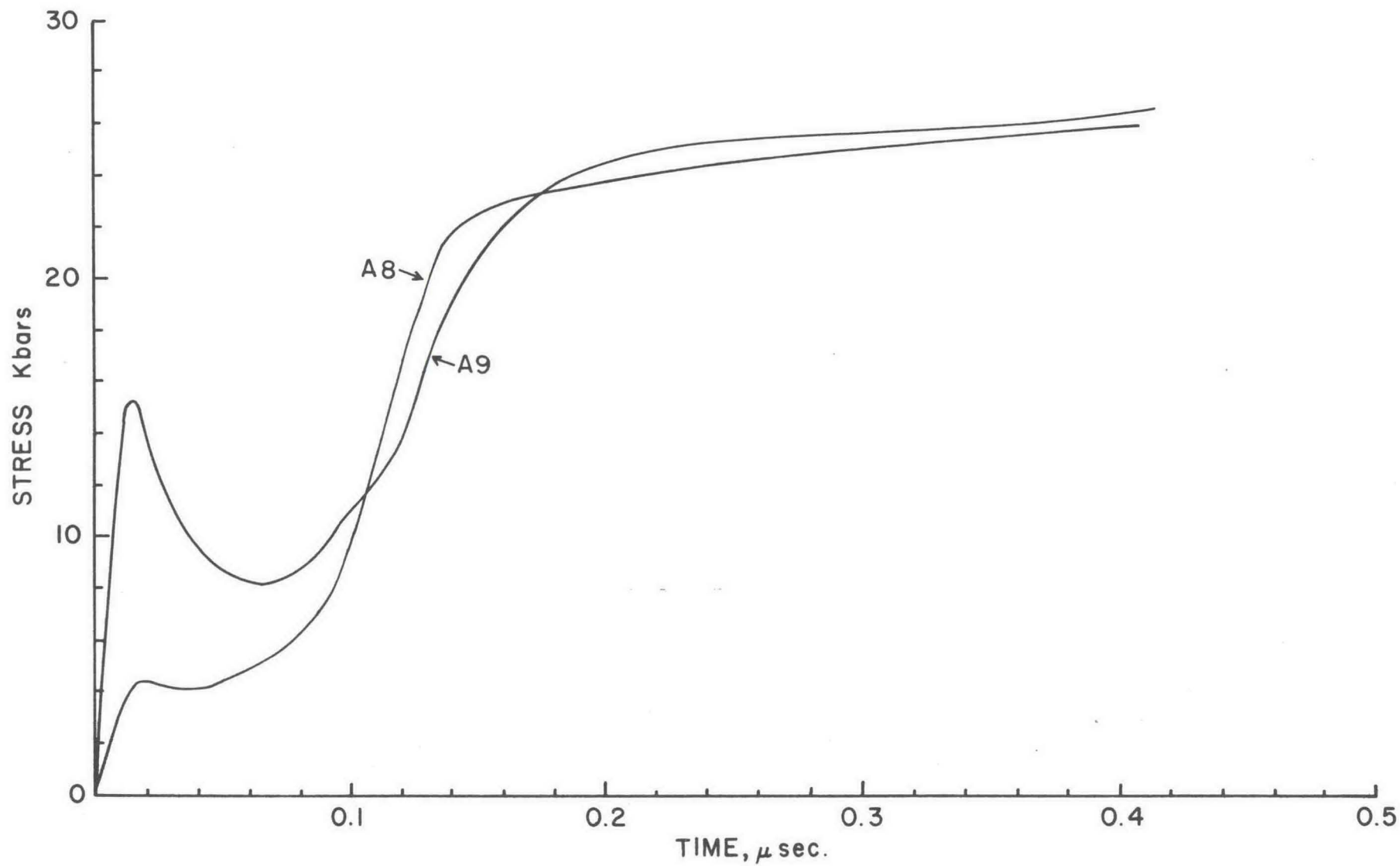


Fig. 27. Stress-time profile for two different specimens of lithium fluoride. The thicknesses of samples A8 and A9 are 2.273 mm and 2.113 mm respectively.

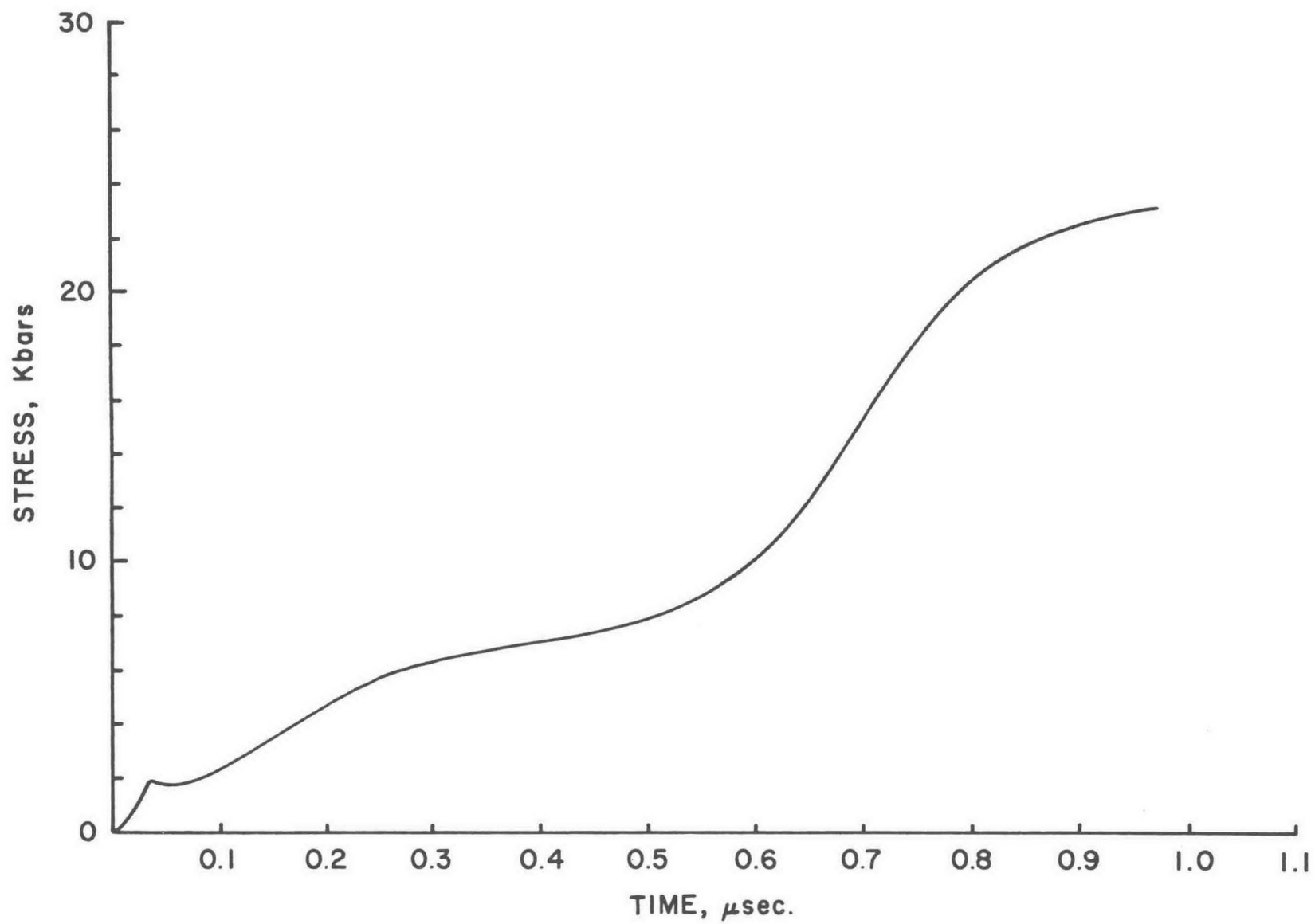


Fig. 28. Stress-time profile for a lithium fluoride sample 15.44 mm in thickness.

C. Magnesium Oxide (MgO)

Magnesium oxide, being a possible constituent of the earth's interior and of value as a high temperature refractory oxide, is of sufficient importance to warrant investigation of its material properties under impact loading. Knowledge of its wave propagation characteristics would be of considerable value to its respective applications. In the single crystal state, it is a brittle transparent solid with a simple sodium chloride structure, similar to LiF. It is hopeful that this simple structure might reduce the complexity of physical models and allow a basic understanding of the processes involved.

Sufficient investigation of the static properties of MgO have been performed to provide the complement necessary for a dynamic investigation. Its hydrostatic equation of state has been extended by Perez-Albuerne et al.²¹ to several hundred kilobars. Plastic yielding and fracture have been examined by Argon et al.²² Dislocation characteristics have been explored and reported.

Of considerable interest is whether brittle materials such as MgO exhibit conventional elastic-plastic behavior typical of more ductile materials. Some dynamic work²³ on MgO indicates that Hugoniot states above the elastic limit fall on or near the hydrostat. However, similar work²⁴ on aluminum oxide appears to show significant offset from the hydrostat implying a residual material rigidity. This difference for apparently similar materials raises doubts as to the applicability of either the fluid model or the elastic-plastic model in describing the physical processes observed. MgO is a reasonable candidate for further exploration of this question. It has a high elastic limit which will make it experimentally favorable. Its stress range of concern allows use of the manganin gauge as a transducer technique.

D. Tungsten (W)

A research program has been undertaken to study elastic precursor attenuation in single-crystal tungsten during shock compression. Tungsten has a body-centered-cubic crystal structure and is

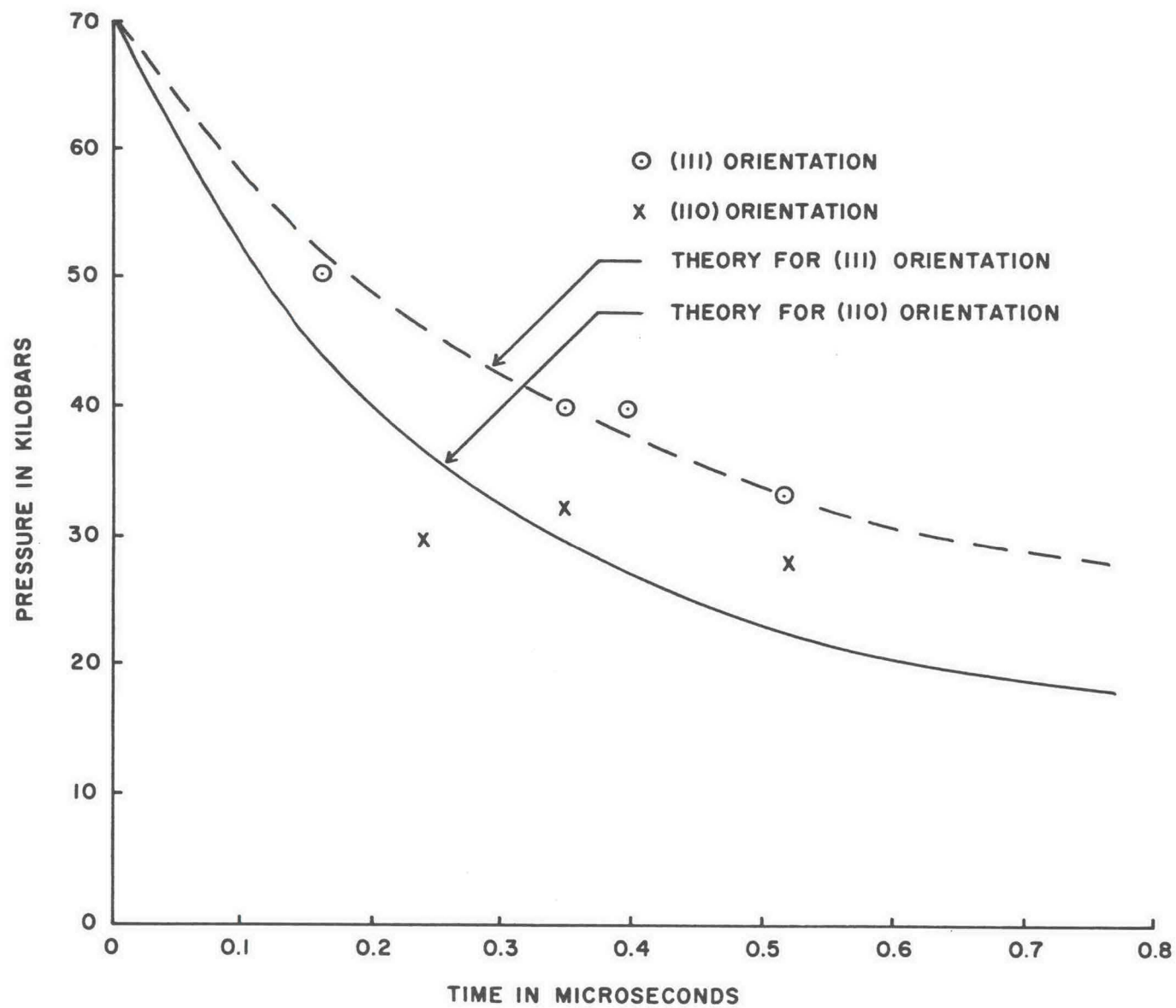


Fig. 29. Decay of elastic precursor wave in tungsten crystals shocked in [111] and [110] direction.

essentially elastically isotropic. The object of this study has been to check experimentally the orientation dependence of elastic precursor attenuation against various proposed theoretical models.^{19, 25} To date seven specimens have been tested to an impact pressure of 70 kilobars. The specimens have been of two orientations, (111) and (110), and of thicknesses ranging from 0.88 mm to 2.78 mm.

The results of these tests have been checked for consistency with a theory developed by Taylor for elastic precursor attenuation that is based upon crystal dislocation dynamics.²⁵ If a dislocation density an order of magnitude greater than initially present in the specimens is assumed, then Taylor's theory and the data obtained thus far are consistent. A similar discrepancy in dislocation density between the initial experimental value and that required for agreement with Taylor's theory has been reported by other investigators.^{19, 26} This discrepancy is possibly due to dislocation multiplication in the elastic wave front or failure of the Gilman relation as a constitutive relation for the dislocation velocities used in Taylor's theory.²⁷ The data are shown in Fig. 29 for the tests conducted thus far along with theoretical curves based on Taylor's theory. The theoretical curves were obtained by using the observed quasi-static slip systems for tungsten at room temperature in Taylor's theory.²⁸ The results are consistent and suggest that, in tungsten, the same slip systems operate at the high strain rates of a shock compression experiment that operate at lower strain rates.

VII. CONCLUSION

The gun facility at WSU is now a reasonably well-equipped and operating laboratory. The performance of the gun is quite satisfactory and staff and students have learned how to operate it and the instrumentation to obtain good experimental data. The higher velocity range, from 0.9 to 1.5 mm/ μ s, has yet to be explored, but no serious problems are anticipated.

It is expected that the research problems now under investigation will lead to advances in fundamental understanding of shock propagation in solids and in the dynamic properties of solids, and that results will begin to become available during the next year.

APPENDIX B

GUN COMPONENTS

FLEX-HOSE

1/4" No. 421 Parker Hose (perforated cover)

VALVES 1/4" PRESSURE: (REMOTE)

Autoclave Engineers Inc. No. 10V4071

Normally closed air operated by light duty operator.

Manual

Same as above only manually operated.

VALVES VACUUM-PRESSURE

1/4" Autoclave Engineers Inc. No. 15SV40718.

Normally closed. Air operated by medium duty operator.

3" Worcestire Economiser Ball Valve No. 411-T-151

Air operated by Kit No. 34C

DUMP TANK

1" 411-T Worcestire Economiser Ball Valve

Air actuated by actuator Fig. 34A.

1" Walworth Valve (Throttle) Fig. 245-P

SOLENOID VALVES TO ACTUATORS

Valcor 55P18C1A (3-way normally closed) 1/4" Npt port 3/16" orifice. 115 VAC 60 cyc. coil.

SOLENOID VALVE (GAS INLET TO PUMP)

Same as above.

HIGH PRESSURE TUBING

Super Pressure Quality 1/4" OD x 7/64" ID

Type 316 SS Tubing. (Autoclave Engineers)

CHECK VALVES

Autoclave Engineers SKO 4400 "O"-ring Check Valve

BOTTLE GAUGES

Marsh 5 DP DFM 2 1/2" Panel Mount

Back Connected 1/4" 0-3000 psi

BREECH GAUGES

ONE 6" Helicoid No. 430 TD

Acaloy Flush Case. 1/4" back connected, shatterproof
lens and blow out discs.

1/4 of 1% accuracy. 0-1500 psi

ONE Same as above only 0-10,000 psi.

RESERVOIR GAUGE

3 1/2" Helicoid No. 410 0-10,000 psi

1/4" back connected, etc.

AIR FILTER

Air Matic Filter No. A602S, 3/4" ports

MICROSWITCH

Allied 1/8 HP. 125V type B2-2RL2-A2

RELAYS

Allied Series KUP55 Industrial Control Relays

10A 120 VAC 3 PDT

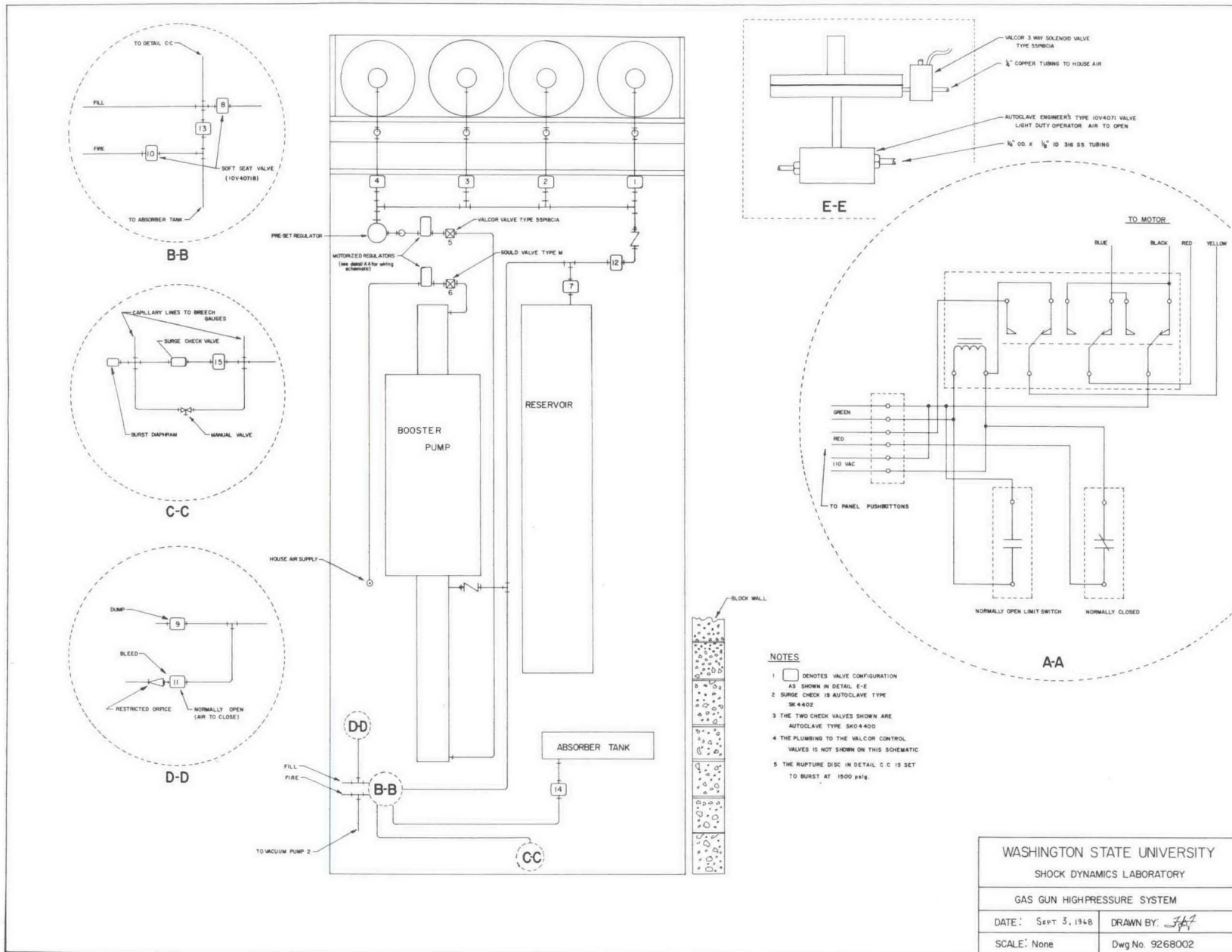
Type KUP 14A55, 41R4S26

PUSH BUTTONS

Molex	SP NC G 1175	8.5 momentary
	SP NO R 1175	8.5 momentary
	SP-R 1175	8.5 push on push off
	SP-R 1175	pilot light
	SP-G 1175	pilot light

PILOT LIGHTS (SCHEMATIC)

Leecraft. 32R 2111T Pilot Light.



REFERENCES

1. Assistance with the design and the construction was provided by Utah Research and Development Co., Salt Lake City, Utah. The barrel and breeches were machined by Clark & Wheeler Engr. Co., Paramount, California.
2. S. Thunborg, Jr., G. E. Ingram and R. A. Graham, "Compressed Gas Gun for Controlled Planar Impacts over a Wide Velocity Range," *Rev. Sci. Instr.* 35, 11 (1964).
3. L. M. Barker and R. E. Hollenbach, "System for Measuring the Dynamic Properties of Materials," *Rev. Sci. Instr.* 35, 742 (1964).
4. Wm. Isbell, G. M. Corp., Warren, Michigan, private communication.
5. A. E. Seigel, "Theory of High Speed Guns," Agardograph 91, U.S. Naval Ordnance Laboratory, Silver Spring, Maryland (1965).
6. R. White, Naval Ordnance Lab., Pasadena, private communication.
7. J. Habberstad, Lawrence Radiation Lab., Livermore, private communication.
8. R. White and R. Fowles, "Effect of Valve Opening Time on Gas Gun Performance," *Rev. Sci. Instr.* 39, #9, 1296 (1968).
9. R. A. Graham, F. W. Neilson and W. B. Benedick, "Piezo-electric Current from Shock Loaded Quartz--A Submicro-second Stress Gauge," *J. Appl. Phys.* 36, 1175 (1965).
10. D. D. Keough and R. F. Williams, "Piezoresistive Transducer for Shock Wave Studies," AFWL-TR-67-81, Air Force Weapons Laboratory, Kirtland AFB, New Mexico (1967).
11. Manufactured by Pacific Photo-Fab, Inc., Mountain View, California.

12. A. N. Dremin and G. A. Adadurov, "The Behavior of Glass under Dynamic Loading," *Soviet Physics-Solid State* 6, 1379 (1964).
13. L. M. Barker, "Fine Structure of Compressive and Release Wave Shapes in Aluminum Measured by the Velocity Interferometer Technique," in Behaviour of Dense Media under High Dynamic Pressures, Symposium H. D. P., p. 483, Gordon and Breech, New York (1968).
14. A. N. Dremin and I. A. Karpukhin, *Zhurnal Prikladnoi Mekhaniki i Tekhnicheskio Fiziki* 3, 184 (1960).
15. S. S. Kabalkina and Z. V. Troitskaya, *Soviet Physics-Doklady* 8, 700 (1964).
16. J. D. Kennedy and W. B. Benedick, *J. Phys. Chem. Solids* 27, 125 (1966).
17. J. W. Taylor, "Dislocation Dynamics and Dynamic Yielding," *J. Appl. Phys.* 36, 3146 (1965).
18. G. E. Duvall, "Propagation of Plane Shock Waves in a Stress-Relaxing Medium," in Stress Waves in Anelastic Solids, Kolsky and Prager, Eds., Springer-Verlag, Berlin (1963).
19. J. M. Kelly and P. P. Gillis, "Dislocation Dynamics and Precursor Attenuation," *J. Appl. Phys.* 38, 4044 (1967).
20. J. J. Gillman, "Microdynamics of Plastic Flow at Constant Stress," *J. Appl. Phys.* 36, 2772 (1965).
21. E. A. Perez-Albuerne and H. G. Drickamer, *J. Chem. Phys.* 43, #4, 1381 (Aug. 15, 1965).
22. A. S. Argon and E. Orowan, *Phil. Mag.* 9, 1023 (1964).
23. T. J. Ahrens, *J. Appl. Phys.* 37, #7, 2532 (June 1966).
24. T. J. Ahrens, *J. Appl. Phys.* 39, #10, 4610 (Sept. 1968)

25. J. W. Taylor, J. Appl. Phys. 36, 3146 (1965).
26. J. N. Johnson, "A Rate-Dependent Constitutive Relation for Polycrystalline Metals," Preprint Sandia Corporation, Albuquerque, New Mexico (1969).
27. J. Asay, private communication.
28. H. W. Schadler, Trans. of Met. Society of AIME, 218, 649 (1960).